Isoscalar short-range current in the deuteron induced by an intermediate dibaryon

V. I. Kukulin and I. T. Obukhovsky
Institute of Nuclear Physics, Moscow State University, RU-119899 Moscow, Russia

Peter Grabmayr
Physikalisches Institut, Universität Tübingen, D-72076 Tübingen, Germany

Amand Faessler
Institut für Theoretische Physik, Universität Tübingen, D-72076 Tübingen, Germany

(Received 11 July 2006; revised manuscript received 13 October 2006; published 26 December 2006)

A new model for short-range isoscalar currents in the deuteron and in the NN system is developed. The model is based on the generation of an intermediate dressed dibaryon, which is the basic ingredient for the medium- and short-range NN interaction proposed recently by the present authors. The new current model has only one free parameter, which has a clear physical meaning. Our calculations have demonstrated that this new current model can very well describe the experimental data for three basic deuteron observables of isoscalar magnetic type: the magnetic moment, the circular polarization of the photon in the $\vec{n}p \to d\vec{\gamma}$ process at thermal neutron energies, and the structure function $B(Q^2)$ up to $Q^2 \simeq 2\,\mathrm{GeV}^2/c^2$.

DOI: 10.1103/PhysRevC.74.064005 PACS number(s): 21.30.Fe, 13.40.−f, 14.20.Pt, 21.10.Ky

I. INTRODUCTION

The problem of electromagnetic currents in the deuteron, especially of an isoscalar nature, still cannot be considered as fully resolved despite numerous and longstanding efforts of many groups. As examples we name here three topics from this field where the present approaches, which all rely on the conventional nucleon-nucleon (NN) force models, failed to explain quantitatively the experimental deuteron data:

(i) the circular polarization P_γ of γ quanta in radiative capture of spin-polarized neutrons in hydrogen at thermal energies [1,2], namely the $\vec{n} + p \to d + \vec{\gamma}$ reaction;
(ii) the deuteron magnetic form factor $B(Q^2)$ around the diffraction minimum at $Q^2_{\min} \sim 50\ \mathrm{fm}^{-2}$ [3–7]; and
(iii) the photon-induced polarization of the neutron from the $d(\gamma, \vec{n})\,p$ reaction at low energy [8].

When going from NN systems to electromagnetic observables of few-nucleon systems disagreements of modern models for two-body currents with existing experimental data become even more numerous. The main part of these discrepancies is related to the isoscalar magnetic currents, which are still strongly model dependent [6–11] and thus cannot be established uniquely. Moreover, in this quest for a remedy, the existing theoretical approaches seem to employ all the important types of currents, namely one-, two-, and three-nucleon ones with many types of meson-exchange currents ($\rho\pi\gamma$, $\omega\pi\gamma$, etc.). Very likely, the various remaining discrepancies could imply that some important contributions to the electromagnetic currents are still absent. These previously ignored current components should remove at least some of the disagreements observed to date in the deuteron and few-nucleon electromagnetic observables.

In the present paper we propose a model for new currents of an isoscalar nature, which have yet to be discussed. It is demonstrated in the following that the new currents remove discrepancies (i) and (ii) and that they make the theoretical framework for electromagnetic properties of the deuteron and the few-nucleon systems more consistent and thus more powerful.

Hence, we shall discuss in Sec. II briefly the status of isoscalar magnetic currents in the deuteron and in the NN system at low energies (see the more extended reviews in Refs. [10–15]). The dibaryon model for the NN interaction is elaborated in Sec. III, where we also include both effective field theory (EFT) and microscopic quark shell-model approaches to substantiate our model. In Sec. IV the properties of the deuteron as emerging from the new force model are discussed in detail. We describe the short-range currents induced by the intermediate dibaryon component and the microscopic quark-model formalism for the deuteron electromagnetic currents. Section V is devoted to a general consideration of the isoscalar $M1$ and $E2$ transition amplitudes and we present in detail the formalism for the calculation of the photon circular polarization in the $\vec{n}p \to d\vec{\gamma}$ process. The numerical results of the new isoscalar magnetic current and their comparison to the respective experimental data are presented in Sec. VI. A summary of the results obtained is given in Sec. VII. In the Appendices some useful formulas and some details of the derivation have been collected.

II. THE STATUS OF ISOSCALAR CURRENTS IN THE DEUTERON

A consistent and correct description of isoscalar currents in the deuteron and in the NN system at very low energy seems to open a door toward quantitative studies of the short-range NN force at low energies, and through this toward to nonperturbative QCD at low energies. At such energies there are no extra difficulties encountered as at high energies (relativistic treatment, incorporation of many

 ©2006 The American Physical Society

inelastic processes, etc.). The problem was first posed by Breit and Rustgi [16] many years ago. The main part of modern efforts to understand the problem quantitatively comes from the EFT treatment in high orders [e.g., next-to-next-to-next-to leading order (N^3LO) and next-to-next-to-next-to-next-to leading order (N^4LO)] and also from the model treatment of short-range NN interaction within phenomenological NN potentials. The point is that the main contribution to the amplitude of processes such as $n + p \to d + \gamma$ comes from the isovector $M1$ current. This two-body current is dominated by a long-range π-meson exchange. The dominance of pion currents is a consequence of the fact that the effective strength of magnetic currents is inversely proportional to the mass of the exchange systems. This phenomenon has been named in the literature as a chiral filter hypothesis [17]. So, the isovector $M1$ transitions are "protected by the chiral filter" and do not manifest any sensitivity to short-range interactions.

In sharp contrast to this picture, the two-body *isoscalar* current is of short-range nature and thus depends sensitively on the short-range interactions. This causes large model dependencies of these currents. As a result, within the framework of the EFT approach the treatment of isoscalar currents requires some higher orders of chiral perturbation theory (ChPT) expansion (N^3LO and N^4LO), which in turn introduce some extra parameters [14,15,18,19]. However, in a more conventional meson exchange currents (MEC) treatment (see, e.g., Refs. [9–12]) the quantitative description of isoscalar currents also includes, in addition to the usual $\rho\pi\gamma$ contribution, the relativistic corrections dependent on the NN interaction model [10,20]. All these contributions depend crucially on the meson-nucleon form factor cutoffs $\Lambda_{\pi NN}$, $\Lambda_{\pi N\Delta}$, $\Lambda_{\rho NN}$, etc. and also on the electromagnetic form factors of the intermediate mesons [10]. It can be noted that the cutoff values Λ chosen to fit the NN elastic scattering are generally much higher than those parameter values needed to describe accurately the *inelastic* channels (e.g., the $p + p \to p + n + \pi^+$ process or the quasi-elastic pion knockout process $p(e, e'\pi^+)n$ [21]) and are also much higher than predictions of all dynamical models for the πNN, ρNN, etc. (see, e.g., the discussions in Refs. [22,23] and further references therein). The clear indication to the strongly enhanced values for the cutoffs $\Lambda_{\pi NN}$, $\Lambda_{\pi N\Delta}$, $\Lambda_{\rho NN}$, etc. chosen in the treatment of electromagnetic processes on the deuteron with traditional NN models such as the Bonn potential model can be seen in the results of relativistic calculations for the deuteron electromagnetic structure functions $A(q^2)$ and $B(q^2)$ and the deuteron magnetic moment [10]. It is very likely that a serious overestimation of the relativistic contributions found in Ref. [10] leads to the too high momentum cutoffs in the meson-nucleon vertices.

Thus, one can summarize that the quantitative treatment of isoscalar currents in existing approaches is related to the rather strong model dependence, in contrast to the isovector $M1$ current. For example, the experimental value for the circular polarization P_γ of γ quanta emitted in the $np \to d\gamma$ process measured some time ago [1] is $P_\gamma^{\rm exp} \simeq (-1.5 \pm 0.3) \times 10^{-3}$ and is underestimated by all existing NN- and two-body current models [24]. Despite some inner inconsistencies in the two-body current models mentioned here the conventional one boson exchange (OBE)-like models are quite successful in the description of many deuteron electromagnetic observables, including static characteristics, charge and quadrupole form factors, and the $np \to d\gamma$ cross sections at low energies. But the description of other electromagnetic observables, in particularly those given in (i)–(iii), meets quite serious difficulties.

In particular, there is a longstanding puzzle that is tightly interrelated to the deuteron isoscalar current: the behavior of the deuteron magnetic form factor $B(Q^2)$ in the area around the diffraction minimum, $Q^2 \sim 45$–55 fm^{-2}. There is a huge literature devoted to calculations of the deuteron form factors. However, the most recent fully relativistic treatment of the $B(Q^2)$ behavior [6,10] has clearly demonstrated that the existing two-body current models have missed some important contributions. Omission of the same contributions is very likely the reason for the visible disagreement of vector and tensor analyzing powers in pd and nd radiative capture at very low energies. Thus, evidentally, there are a number of mutually interconnected effects in the deuteron and in the few-nucleon systems where one needs a new isoscalar current. However, the conventional two-body current models still have no appropriate candidates for this current.

In this paper we propose an alternative mechanism for the isoscalar current generation in the two-nucleon system based on the dibaryon model for NN interactions at intermediate and short ranges developed recently by our group [23,25–27]. Generally speaking, the employment of the dibaryon degree of freedom to describe quantitatively the electromagnetic deuteron properties at low energies is not new. As an example, we shall refer to numerous studies having appeared in the 1980s where authors tried to incorporate various types of six-quark bags to the deuteron wave function to explain some puzzles observed in electromagnetic observables (see, e.g., Refs. [28–32]). These early attempts have revealed the important role that the quark degrees of freedom play in the short-range NN interaction and in the electromagnetic structure of the deuteron (see, e.g., Ref. [32] and references therein). The great importance of a "hidden color" and of the quark pair currents in the deuteron electromagnetic form factors has been established in these works, in particular. However, these early attempts did not lead to significant improvement in the description of experimental data.

Very recently, however, in tight interrelation to a renaissance of dibaryon physics (which is related partially to a recent boom in pentaquark physics), many new studies, both theoretical [33–39] and experimental [40–42], have appeared in the literature. An EFT approach that included intermediate dibaryons [37–39] focused just on the description of electromagnetic properties of the deuteron at low energies and momentum transfer. However, the dibaryons in that approach have been introduced more on a formal basis than as a real physical degree of freedom (or an intermediate broad resonance), to improve the convergence of chiral perturbation series and to simplify the EFT scheme in that case. In our dibaryon approach, in contrast to the formal scheme [33–36], the dibaryons are considered as an important new degree of freedom in the description of NN and $3N$ interactions in nuclei at intermediate and short ranges [23,25,27].

The dibaryon concept of the nuclear force at intermediate and short ranges turned out to be very fruitful in a quantitative or qualitative description of some phenomena in hadron and nuclear physics. In particular, this model made it possible to explain without any free parameter the Coulomb displacement energy for $A = 3$ nuclei, ^{3}H and ^{3}He, and all their ground-state characteristics [43] (with the exception of the ^{3}H and ^{3}He magnetic moments where we included only single-nucleon currents). Moreover, according to a general principle of quantum mechanics, any new degree of freedom leads to new currents of diagonal and transitional type. However, in our approach the weight of the dibaryon component in the deuteron does not exceed 2.5–3.5%. Therefore, just the transitional current from the NN to the dibaryon component can be more important than the diagonal dibaryon current. Nevertheless, we have considered in the present study the diagonal dibaryon current as well.

III. THE DRESSED BAG MODEL FOR THE MEDIUM- AND SHORT-RANGE NN INTERACTION

A few key points have been taken as the physical justification of this dibaryon model:

(i) It fails to explain the intermediate-range attraction in the NN channel in terms of the exchange of two correlated pions [44–46] (in contrast to traditional phenomenological approaches with the NN attraction generated by exchange of the σ meson as an elementary particle). Instead of a strong attraction required by the NN phase shifts, the exchange of two correlated pions with the S-wave broad resonance in $\pi\pi$ scattering included in the mechanism, when treated consistently and with rigor, leads to a strong medium-range *repulsion* and a weak long-range attraction [45,46]. Thus, the crucial problem arises as to how to explain the basic strong attraction between two nucleons at intermediate range.

(ii) The heavy-meson exchange with the mass $m_{\rho,\omega} \sim 800$ MeV corresponds in general to the internucleon distances $r_{NN} \sim 0.3$ fm (i.e., it occurs deeply inside the overlap region between two nucleons). And thus, these exchanges should be consistently treated only with invoking six-quark dynamics. Ignoring this dynamics in conventional NN-potential approaches (of OBE type) leads to several serious inconsistencies in the OBE description of short-range NN force (see the discussion in Refs. [23,25,47]) and is also a reason for some problems with the description of the short-range NN correlations in nuclei.

(iii) One more serious difficulty is related to the choice of different cutoff parameter values $\Lambda_{\pi NN}, \Lambda_{\pi N\Delta}$, etc., when one set is used to describe the elastic NN scattering, another set is used to fit the pion production cross section in NN scattering and the meson-exchange contribution to the two-body current, and a third set is used to describe the three-body force [11,23,25]. Using these different values for the identical vertices in the description of tightly interrelated quantities points toward an inadequate framework employed in the underlying model.

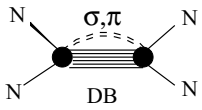

FIG. 1. Driving mechanism for the dressed dibaryon generation used as an intermediate state in the NN interaction.

The dibaryon model [25,27] seemingly overcomes these difficulties with a consistent description of the short-range NN force. First, it employs a rather soft cutoff parameter $\Lambda_{\pi NN}$. (Moreover, there is likely no serious sensitivity to these cutoffs in our model.) Second, the short-range NN interaction is described through dressed dibaryon dynamics, so that the conventional heavy-meson exchange in the t channel plays no serious role in the short-range NN dynamics. Third, the short-range NN correlations in nuclei tested by high-energy probes can consistently be described as an interaction of the probes with the dibaryon as a whole, which may be associated with its inner excitations or de-excitations.

In our approach the virtual dibaryon in the NN system is modeled through generation of a symmetric six-quark configuration $s^6[6]_X$ dressed with a strengthened scalar (e.g., σ meson) and other (e.g., π, ρ, ω, etc.) fields, as schematically illustrated in Fig. 1. The enhancement of the scalar field in the symmetric six-quark configuration $s^6[6]_X$ implies some rearrangement of quark-gluon fields in the region, where two nucleons are totally overlapping. The emergence of a strong scalar-isoscalar field in the six-quark bag induces automatically an isoscalar exchange current in the multiquark system.

The σ-meson loops originate mainly from "nondiagonal" transitions from the mixed-symmetry $2\hbar\omega$-excited configurations $|s^4p^2[f_X][f_{CS}]\rangle$ to the unexcited fully symmetric configuration $|s^6[6_X]\rangle$ in the six-quark system with emission of a (virtual or real) σ meson. In turn, the strongly attractive interaction between the scalar-isoscalar σ field and the multiquark bag results in an enhancement of the attractive very short range diquark correlations in the multiquark system. Thus, as a net result of all these highly nonlinear effects the mass of the intermediate dibaryon surrounded by the σ field gets much lower as compared to the respective bare dibaryon (see the discussion in the following).

Completely similar to the behavior of the nucleonic system in a scalar field, where the scalar exchange may be viewed as a renormalization of the nucleon mass [48]

$$m \to m^* = m + v_s(0)\rho,$$

where $v_s(0)$ is a volume integral of the scalar exchange potential and ρ is the nucleon density, the constituent quark mass in the multiquark system is also reduced owing to interaction with the scalar field $v_s(0) \sim -g_{\sigma q}^2/m_\sigma^2$, where $g_{\sigma q}$ is the σ-quark coupling constant; note that $v_s(0) < 0$. Thus, the dibaryon mass should be renormalized noticeably because of this scalar field mechanism.

The effect of the strong attraction of the σ field to the quark core and the resulting mass shift of the multiquark system is illustrated easily by the anomalously low mass of the Roper resonance $N^*(1440)$ with positive parity, which

lies even lower than the lowest negative-parity resonance $N^*(1535)$. It is widely accepted [47] that the Roper reson ance has mainly the structure $|N+\sigma\rangle$. However, in the language of the simple quark shell model, the second positive-parity level in the nucleon spectrum corresponds to $2\hbar\omega$-excited three-quark configurations $|sp^2[21]_X\rangle$ or $|s^2d - (s^2 2s)[21]_X\rangle$. Thus, exactly the same mechanism as in our dibaryon model (i.e., the σ-meson emission from the $2\hbar\omega$-excited state of the nucleon $|sp^2[21]_X\rangle \to |s^3[3]_X + \sigma\rangle$) leads to a generation of a strong σ field and to a significant shift downward of the Roper resonance mass. Without this strong nonlinear effect, the mass of the $N^*(1440)$ would be $\sim$500 MeV higher than that found experimentally. This very large shift gives some estimate for the magnitude of the attractive effects that appear in the interaction of the scalar field with the fully symmetric multiquark bag, or in other words, the effect of dressing by the σ-meson field. At very short NN distances the qq correlations become repulsive owing to one-gluon exchange, and, jointly with a strongly enhanced quark kinetic energy, this results in effective short-range repulsion in the NN channel. In our approach this repulsive part of the nonlocal NN interaction is modeled by a separable term $\lambda_0\varphi_{0S}(\mathbf{r})\varphi_{0S}(\mathbf{r}')$ with a large positive coupling constant λ_0 [23,25] whereas the form factor $\varphi_{0S}(\mathbf{r})$ is the projection of the six-quark $|s^6[6]_X\rangle$ state onto the NN channel: $\varphi_{0S}(\mathbf{r}) = \langle N\,N|s^6[6]_X\rangle$.

Such a combined mechanism lies fully beyond perturbative QCD, and we suggest it can be described phenomenologically by dressing the six-quark propagator $G_{6q}(E)$ with σ-meson loops [26,27]. The resulting dressed bag (DB) propagator $G_{\rm DB}(E)$ and the transition vertices $NN \to$ DB and DB$\to NN$ treated within a microscopic $6q$ model [25] lead automatically to a nonlocal (separable) energy-dependent short-range NN potential $V_{NqN}(r, r'; E)$:

$$V_{NqN} \equiv \langle NN|V_{Nq}|{\rm DB}(s^6)\rangle G_{\rm DB}(E)\,\langle {\rm DB}(s^6)|V_{qN}|NN\rangle = \varphi(r)\lambda(E)\varphi(r'), \quad (1)$$

where the form factors $\varphi(r)$ are deduced from the microscopic $6q$ model and the coupling constant $\lambda(E)$ is determined by a loop integral with the σ loop as shown schematically in Fig. 1 [25]. This loop integral can be conventionally parametrized in the following Pade form:

$$\lambda(E) = \lambda(0)\frac{E_0 + aE}{E_0 - E}. \quad (2)$$

Here the parameters $\lambda(0)$, E_0, and a can be either calculated from the microscopic $6q$ model or obtained from fits to the phase shifts of NN scattering in the low partial waves. This approach resulted in the Moscow-Tuebingen (MT) potential model of NN interaction [23,25].

In a more general treatment recently developed in Refs. [26,27] the one-pole approximation for V_{NqN} was obtained on the basis of a fully covariant EFT approach. In a more simple version of the model [23,25] the transition operator V_{Nq}, which couples the nucleon-nucleon and dibaryon channels, was calculated within a microscopic quark model with employment of the quark-cluster decomposition of the short-range NN wave function. We consider here the $NN \to$ DB transition

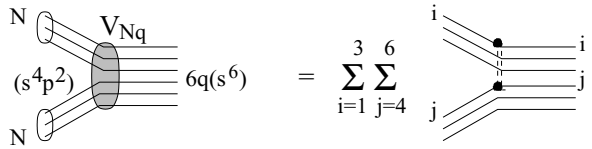

FIG. 2. Graphical illustration for $NN \to$ DB transition in terms of the quark model. The double-dashed line denotes a scalar exchange that can induce the $NN \to$ DB transition [26,27].

in terms of this simple model, shown schematically in Fig. 2, where we assume that the coupling between the NN and DB channels is realized on the quark level via a scalar exchange. This scalar interaction can be presented not only through the σ-meson exchange but also through a quark confinement or another force including even the four-quark instanton-induced interaction of t'Hooft's type [49].

The transition operator V_{Nq} can be written in the form

$$V_{Nq} = \sum_{i=1}^{3}\sum_{j=4}^{6} g_s^2 v_s(r_{ij}), \quad (3)$$

where $v_s(r_{ij})$ is a scalar qq interaction. This operator should be substituted into the transition matrix element in Eq. (1). The particular form of the scalar operator (3) and its origin are not significant here. The specific mechanism of dressing can also be disregarded at this step since the dressing has already been taken into account in the propagator $G_{\rm DB}$. The most important point is that the S-wave two-cluster state $3q + 3q$, which represents the NN system in the overlap region, should be very close in its symmetry to a superposition of the excited six-quark configurations s^4p^2 (see Refs. [50,51] for additional details) having nontrivial permutation symmetries with the following Young tableaux in the coordinate and color-spin spaces $\{f\} \equiv \{[f_X], [f_{CS}]\}([f_X] = [6],\ [42],\ [f_{CS}] = [42],\ [321],\ [2^3],\ [31^3],\ [21^4])$. For this reason, we can rewrite the effective NN interaction [Eq. (1)] generated by the transition operator [Eq. (3)] in the following constrained form:

$$V_{NqN}(r, r'; E) \simeq \sum_{ff'}\{\langle N(123)|\langle N(456)|\}|s^4p^2\{f\}\rangle \times \langle s^4p^2\{f\}|V_{Nq}|s^6[6]_{\rm X}\rangle \times G_{\rm DB}(E)\,\langle s^6[6]_{\rm X}|V_{Nq}|s^4p^2\{f'\}\rangle \times \langle s^4p^2\{f'\}|\,\{|N(123)\rangle|N(456)\rangle\}, \quad (4)$$

where we leave the mixed-symmetry $2\hbar\omega$-excited six-quark configuration s^4p^2 only (but with all the possible Young tableaux $\{f\}$), instead of the total sum over all the excited six-quark configurations $s^4p^2, s^2p^4, \ldots$, etc. Then, one can deduce from Eq. (4) that the matrix element of the $NN \to$ DB transition is proportional to the wave function of an *excited* nucleon-nucleon $2S$ state:

$$\{\langle N(123)|\langle N(456)|\}\,|\,s^4p^2\{f\}\rangle = C_f\,\varphi_{2S}(r). \quad (5)$$

Here the C_fs are purely algebraic coefficients and $\mathbf{r} = (\mathbf{r}_1 + \mathbf{r}_2 + \mathbf{r}_3 - \mathbf{r}_4 - \mathbf{r}_5 - \mathbf{r}_6)/3$ is the relative-motion coordinate of the two $3q$ clusters. For simplicity, we use here the harmonic oscillator (h.o.) $2S$-state function $\varphi_{2S}(r) =$

$2r_0^{-3/2}\pi^{-1/4}\sqrt{3/2}(2r^2/3r_0^2 - 1)\exp(-r^2/2r_0^2)$ for the projection of the mixed-symmetry six-quark state onto the NN channel, which is characteristic of the quark shell model. In a more general treatment, some higher $6q$ shell-model configurations such as s^2p^4 and p^6 should also be added in the NN-$6q$ overlap functions in Eq. (4). But these higher components play a minor role in the NN interaction and can be seen only in the NN charge operator at high momentum transfer (see the respective estimates in Appendix C). The nucleon wave function $N(ijk)$ in such an approach is described by the pure s^3 configuration of the constituent quark model (CQM)

$$|N(123)\rangle = |s^3[3]_X\{f_{ST}\}\rangle = \psi_N(\rho_1, \rho_2)|[2^3]_C[3]_{ST}\rangle, \quad (6)$$

where $\psi_N(\rho_1, \rho_2) = \mathcal{N}\exp[-\frac{1}{2b^2}(\rho_1^2/2 + 2\rho_2^2/3)]$, and the parameter b is the scale parameter of the CQM, with $b \simeq 0.5$–0.6 fm; the relative coordinates are $\boldsymbol{\rho}_1 = \mathbf{r}_1 - \mathbf{r}_2$ and $\boldsymbol{\rho}_2 = (\mathbf{r}_1 + \mathbf{r}_2)/2 - \mathbf{r}_3$.

Then, using the $2S$ function for the transition $NN \to$ DB vertex in Eq. (1) [i.e., substituting $\varphi(r) = \varphi_{2S}(r)$], we obtain in our simple ansatz [Eq. (3)] for the qq pair interaction $v_s(r_{ij})$

$$\langle NN(s^4p^2)|V_{Nq}|\mathrm{DB}(s^6)\rangle = g_s^2\,\langle v\rangle\,\varphi_{2S}(r), \quad \text{and} \quad \lambda(E) = g_s^4\,\langle v\rangle^2 G_{\mathrm{DB}}(E), \quad (7)$$

where $\langle v\rangle$ is a superposition (with the algebraic coefficients C_f) of the quark shell-model *transition matrix elements* $\langle s^4p^2|\sum_{i=1}^3\sum_{j=4}^6 v_s(ij)|s^6\rangle$.

Note that we did not include the projector $|s^6[6]_X\rangle\langle s^6[6]_X|$ onto the lowest six-quark configuration $s^6[6]_X$ in the sum within Eq. (4), because this configuration, according to the most recent $6q$ calculations [52], lies well above 2.5 GeV and it is not touched by a strong renormalization, as the mixed-symmetry state does because of its strong coupling to the σ-meson field. Thus, the strong repulsive contribution from the bare intermediate s^6 bag to the effective short-range NN interaction in the MT model [23,25] is modeled by an orthogonality condition to the nodeless $0S$ state:

$$\int \psi_{NN}(r)\varphi_{0S}(r)d^3r = 0, \quad (8)$$

where φ_{0S} is a projection of the $6q$ bag state onto the product of nucleon wave functions:

$$\varphi_{0S}(r) = \mathcal{N}_0^{-1}\langle N(123)|\{|N(456)|\}|s^6[6]_X\rangle. \quad (9)$$

Through the orthogonality constraint (8) and (9) the symmetric six-quark bag configuration is excluded from the NN Hilbert space, which prevents a possible double counting of the s^6 configuration. As a result, the total wave function of the two-nucleon system Ψ_{tot} is defined in the direct sum of two Hilbert spaces $\mathcal{H}_{NN} \oplus \mathcal{H}_{\mathrm{DB}}$. This direct sum can be conventionally represented by the two-line Fock column. For example, the deuteron state in the MT model reads

$$|d\rangle = \begin{pmatrix} \cos\theta_{Nq}|d(NN)\rangle \\ \sin\theta_{Nq}|\mathrm{DB}\rangle \end{pmatrix}, \quad (10)$$

where the mixing angle θ_{Nq} is calculated on the basis of coupled-channel equations with the transition operator V_{Nq} taken as a coupling potential [43]. Here the deuteron wave function in the NN channel (or the NN component of the deuteron) takes the conventional form

$$|d(NN)\rangle = \frac{u(r)}{r}\mathcal{Y}_{1M}^{01}(\hat{r}) + \frac{w(r)}{r}\mathcal{Y}_{1M}^{21}(\hat{r}), \quad (11)$$

where the S-wave component $u(r)$ satisfies the constraint

$$\int_0^\infty u(r)\varphi_{0S}(r)dr = 0. \quad (12)$$

The deuteron NN component $|d(NN)\rangle$ and the dibaryon component $|\mathrm{DB}\rangle$ are normalized individually to 1. This implies a standard normalization of the total wave function

$$\langle d|d\rangle = \cos^2\theta_{Nq}\langle d(NN)|d(NN)\rangle + \sin^2\theta_{Nq}\langle \mathrm{DB}|\mathrm{DB}\rangle = 1. \quad (13)$$

The dressed dibaryon propagator $G_{\mathrm{DB}}(E)$ can be represented through the Dyson equation

$$G_{\mathrm{DB}} = G_{\mathrm{DB}}^{(0)} + G_{\mathrm{DB}}^{(0)}\Sigma G_{\mathrm{DB}}, \quad (14)$$

where $G_{\mathrm{DB}}^{(0)}$ is the bare dibaryon propagator and Σ is an eigenenergy that includes irreducible diagrams, that is, those that do not include the intermediate free nucleon lines (but still can include $N\Delta$ or $\Delta\Delta$ channels). Our DB-model calculations kept only the leading σ loop [26,27] in the series for the Σ kernel, because all other graphs (calculated within the six-quark shell model for the quark bag) correspond to much higher masses (for details see Refs. [26,27]). Moreover, the propagator for the bare six-quark bag $G_{\mathrm{DB}}^{(0)}$ corresponds to the pure six-quark bag states with $0\hbar\omega$ and $2\hbar\omega$ quanta for even partial waves and $1\hbar\omega$ for odd partial waves.

When including the σ-meson loops only into the dressing mechanism, the dressed bag propagator in the one-pole approximation takes the form [25,43]

$$[G_{\mathrm{DB}}]_{LL'}^J = \int d\mathbf{k}\frac{B_L^J(\mathbf{k})B_{L'}^J(\mathbf{k})}{E - E_\alpha(\mathbf{k})}, \quad (15)$$

where $B_L^J(\mathbf{k})$ is the σDD form factor and $E_\alpha(\mathbf{k})$ is the total energy of the dressed bag [in the nonrelativistic case $E_\alpha(\mathbf{k}) \simeq m_\alpha + \varepsilon_\sigma(\mathbf{k})$, with $\varepsilon_\sigma(\mathbf{k}) = k^2/2m_\alpha + \omega_\sigma(\mathbf{k}) \simeq m_{\sigma\alpha} + k^2/2m_\sigma$, and $m_{\sigma\alpha} = m_\sigma m_\alpha/(m_\sigma + m_\alpha)$ whereas $\omega_\sigma = \sqrt{m_\sigma^2 + k^2}$ is the relativistic energy of σ meson]. Thus the effective interaction in the NN channel induced by the intermediate dressed dibaryon production takes the following form in the partial-wave representation:

$$V_{NqN} = \sum_{JLL'} W_{LL'}^J(\mathbf{r}, \mathbf{r}'; E), \quad (16)$$

with

$$W_{LL'}^J(\mathbf{r}, \mathbf{r}'; E) = \sum_M \varphi_L^{JM}(\mathbf{r})\lambda_{LL'}^J(E)\varphi_{L'}^{JM}(\mathbf{r}'), \quad \lambda_{LL'}^J(E) = \gamma^2[G_{\mathrm{DB}}]_{LL'}^J, \quad (17)$$

where $\gamma^2 = g_s^4\langle v\rangle^2$ [see Eqs. (4)–(7) for comparison].

It is easy to show [25,43] that the weight of the DB in the total NN wave function in the $LL'SJ$ channel is proportional

to the energy derivative,

$$\beta^2_{LL'J} = -\frac{\partial \lambda^J_{LL'}(E)}{\partial E}. \tag{18}$$

This derivation is in close analogy to a similar procedure for the weight of the dressed particle state by using the energy derivative of the respective polarization operator $\Pi(P^2)$ in the field-theory formalism. In particular, recently we developed the fully covariant EFT derivation [26,27] for the relativistic NN potential at intermediate and short ranges, similar to Eqs. (15)–(18); we also derived in the simplest one-state approximation a separable form for the relativistic NN interaction in channels $^1S_0$ and $^3S_1$-$^3D_1$, which fits almost perfectly the respective NN phase shifts for the large energy interval 0–1000 MeV. In contrast to other potentials (e.g., the purely phenomenological Graz separable NN potential, which includes a few dozen adjustable parameters for a smaller energy interval) this high-quality fit has been performed using only four parameters in the singlet $^1S_0$ channel and a few more for the coupled-channel case $^3S_1$-$^3D_1$.

The separable form of the short-range NN interaction given in Eqs. (16) and (17) can be clearly compared to the contact terms in the EFT approach (pionless) where all the high-energy physics is parametrized via some contact terms (see the left graph of Fig. 3), which cannot be calculated within that low-energy approach and must be either parametrized somehow phenomenologically or fitted to the data [26,27]. However, our short-range mechanism (shown schematically in the right graph of Fig. 3) gives just the energy dependence for such contact terms.

IV. DEUTERON STRUCTURE AND DIBARYON-INDUCED SHORT-RANGE CURRENTS

Similar to the general description of the NN system given in Sec. III the total deuteron wave function in the DB model has the form of the Fock column [Eq. (10)] with at least two components, the NN and the dibaryon dressed with a σ field—a dressed bag [23,25]. The DB component $|\mathrm{DB}\rangle$ in the second line of Eq. (10) can be presented in the graphic form as a superposition of a bare dibaryon (six-quark configuration $s^6[6_X]$) and an infinite series of σ-meson loops coupled to the s^6-quark core propagator. Thus, this component includes both the bare and dressed parts.

Taking further the simple Pade form (2) of the energy-dependent factor $\lambda^J_{LL'}(E)$ in Eq. (17) and by calculating the energy derivative (18) one gets easily the weight of the dressed

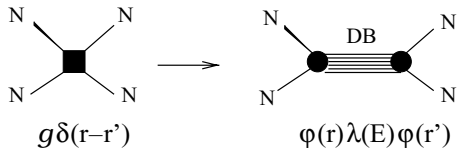

FIG. 3. Different ways for parametrizing the short-range NN interaction: in low-energy (pionless) EFT through the four-nucleon contact term (left) and in the dibaryon model (right) via the s-channel intermediate dibaryon.

dibaryon component in the deuteron, which turns out to be $\beta^2 \simeq 0.025$–0.035 for different versions of the model. It is very interesting that this weight of the dibaryon component derived from the energy dependence of the σ-loop diagram is rather close to the weight of non-nucleonic components (e.g., $\Delta\Delta$) in the deuteron deduced within many phenomenological models. Table I gives the summary of the static characteristics of the deuteron found with this dibaryon model [25,60].

The parameters of the model obtained from a fit to the phase shifts of elastic NN scattering in the $^3S_1$-$^3D_1$ channel have the following values:

$$\lambda(0) = -385.89\,\mathrm{MeV}, \quad E_0 = 855.29\,\mathrm{MeV},$$
$$a = -0.025, \quad r_0 = 0.38113\,\mathrm{fm}, \quad b = \sqrt{\frac{3}{2}}r_0. \tag{19}$$

We emphasize here again that after fitting the phase shifts our approach does not have any free or adjustable parameters left for the description of the deuteron properties. From Table I one can see that the predictions for the basic deuteron observables found in this dibaryon model are generally even in better agreement with respective experimental data than those for the modern NN potentials found within the conventional force models.

A more severe test of the deuteron structure at intermediate and short distances can be performed on the deuteron charge and quadrupole form factors at large Q^2. To this end, we have calculated both form factors within the framework of our dibaryon model using the nucleonic currents in the deuteron. In Figs. 4(a) and 4(b) we compare our predictions with results of other modern NN potential models. It is evident that for charge and quadrupole form factors the dibaryon model predictions are in quite good agreement with results of other potential models. Further improvement for $G_c(Q)$ at $Q > 4$ fm^{-1} can be reached by passing to its relativistic treatment [10] and by incorporation of the MEC contributions for the charge within the present model, which will be considered in our subsequent paper.

Our main focus in the present study is on the magnetic properties of deuteron, which can be interrelated closely to the coupling of the intermediate dressed dibaryon with the external electromagnetic field. The modeling of the $NN \to$ DB transition by scalar exchanges between quarks makes it possible to consider the "contact" $\gamma NN \to$ DB vertices (Fig. 5) in terms of the CQM with the minimal electromagnetic interaction of the constituent quarks, that is, with the quark current

$$j^\mu_q(q) = \sum_{i=1}^{6} \hat{e}_i F_q(q^2) \bar{u}(p'_i)\gamma^\mu_i u(p_i), \tag{20}$$

where $q = p' - p$, $\hat{e}_i = \frac{1}{6} + \frac{1}{2}\tau^{(i)}_z$, and $F_q(q^2)$ is a form factor of the constituent quark, which can only show itself at intermediate momentum transfer $Q^2 \gtrsim 1$ GeV$^2/c^2$. The model implies that the constituent quark is an extended object and should be characterized by its own electromagnetic form factor, for example, a monopole one $F_q(Q^2) = 1/(1 + Q^2/\Lambda^2_q)$, where the parameter Λ_q is expected to be set by the chiral symmetry scale $\Lambda_\chi \simeq 4\pi f_\pi \simeq 1$ GeV.

TABLE I. Deuteron properties in different models.

Model	E_d (MeV)	P_D (%)	r_m (fm)	Q_d (fm^2)	μ_d (μ_N)	A_S (fm$^{-1/2}$)	D/S
RSC	2.22461	6.47	1.957	0.280	0.8429	0.8776	0.0262
AV18	2.2245	5.76	1.967	0.270	0.8521	0.8850	0.0256
Bonn 2001	2.22458	4.85	1.966	0.270	0.8521	0.8846	0.0256
DB (NN only)	2.22454	5.42	2.004	0.286	0.8489	0.9031	0.0259
DB ($NN+6$q)	2.22454	5.22	1.972	0.275	0.8548	0.8864	0.0264
Experiment	2.22454(9)[a]		1.971(2)[b]	0.2859(3)[c]	0.857406(1)[d]	0.8846(4)[e]	0.0264[f]

[a]Reference [53].
[b]Reference [54].
[c]References [55] and [56].
[d]Reference [57].
[e]Reference [58].
[f]Reference [59].

For definiteness, we consider diagrams (a) and (c) depicted in Fig. 5. In our model with the scalar exchanges and the CQM current [Eq. (20)] these contact terms are equivalent to the sum of Feynman diagrams depicted in Fig. 6. These diagrams describe the two-particle currents in the six-quark system. Diagram (e) in Fig. 6 gives rise to an additional (i.e., the γ-induced) contribution to the transition $s^4p^2 \to s^6$ as compared to the mechanism shown in Fig. 2. Here we demonstrate that within our model for the short-range NN interaction the minimal quark-photon coupling $j_q^\mu(q)A_\mu(q)$ leads to a nonadditive two-nucleon current that does not vanish in the low-energy limit $q_0, |\mathbf{q}| \to 0$. In this limit, only the contribution of the diagram in Fig. 6(e) vanishes because of orthogonality of the s^6 configuration to the quark-cluster states in the NN channel (i.e., to the configurations s^4p^2 and the other ones). By contrast, the total contribution of diagrams (a)–(d) and (f) in Fig. 6 does not vanish as $q_0 \to 0$. In each pair of diagrams, (a) and (b), depicted in Fig. 7, the singular terms $\sim 1/q_0$ are mutually canceled, but the remainder, proportional to the momentum $\mathbf{k}$ between the ith and jth quarks and also to the scalar qq interaction potential $v_s(\mathbf{k}^2)$, does not vanish in the limit $q_0 \to 0$ because of the nonvanishing matrix element $\langle s^4p^2|v_s|s^6\rangle$ (see the following).

Now we pass to the actual calculations of such diagram contributions. It should be stressed here that the current diagrams in Fig. 6 correspond just to the "nondiagonal" (transition) electromagnetic current, which couples two different channels (i.e., the proper NN and the DB channels). These channel wave functions enter the transition matrix elements with a proper normalization because any current associated with the DB state is "normalized" to the weight of the DB component. Among other things this makes it possible to avoid any double counting. (The symmetry properties of quark configurations, discussed in Appendix C, argue strongly against the repeated contribution.) When the spin part of the ith quark current [Eq. (20)] is taken into account only and a low-energy $M1$ photon is generated, one can write the following Feynman amplitudes M_{ij}^λ for the diagrams depicted in Figs. 7(a) and 7(b):

$$M^\lambda_{ij(a)} = \frac{ieg_s^2 v_s(k_j^2)}{2m_q}\bar{u}(p_i')\left\{\hat{e}_i\sigma_i^{\mu\nu}q_\nu\varepsilon_\mu^{(\lambda)*}\frac{2m_q - \not{k}_i + \not{q}}{2p_i'q} + \frac{2m_q + \not{k}_i - \not{q}}{-2p_iq}\hat{e}_i\sigma_i^{\mu\nu}q_\nu\varepsilon_\mu^{(\lambda)*}\right\}u(p_i),$$
$$M^\lambda_{ij(b)} = \frac{ieg_s^2 v_s(k_i^2)}{2m_q}\bar{u}(p_j')\left\{\hat{e}_j\sigma_j^{\mu\nu}q_\nu\varepsilon_\mu^{(\lambda)*}\frac{2m_q - \not{k}_j + \not{q}}{2p_j'q} + \frac{2m_q + \not{k}_j - \not{q}}{-2p_jq}\hat{e}_j\sigma_j^{\mu\nu}q_\nu\varepsilon_\mu^{(\lambda)*}\right\}u(p_j), \quad (21)$$

where $\varepsilon_\mu^{(\lambda)*}$ is a spacelike photon polarization vector $\varepsilon^{\mu(\lambda)*} = \{0, \boldsymbol{\epsilon}^{(\lambda)*}\}$ satisfying the transversality condition $\hat{\mathbf{q}}\,\boldsymbol{\epsilon}^{(\lambda)*} = 0$ at $\lambda = \pm 1$.

It is easy to verify that the singular terms $\sigma_i^{\mu\nu}q_\nu\varepsilon_\mu^{(\lambda)*}m_q/(p_i'q)$ and $\sigma_i^{\mu\nu}q_\nu\varepsilon_\mu^{(\lambda)*}m_q/(-p_iq)$ cancel each other in the sum $M^\lambda_{ij(a)} + M^\lambda_{ij(b)}$ in the limit $q_0 \to 0$. As a result, we obtain from Eq. (21) in the nonrelativistic approximation $q_0/m_q \ll 1$ the

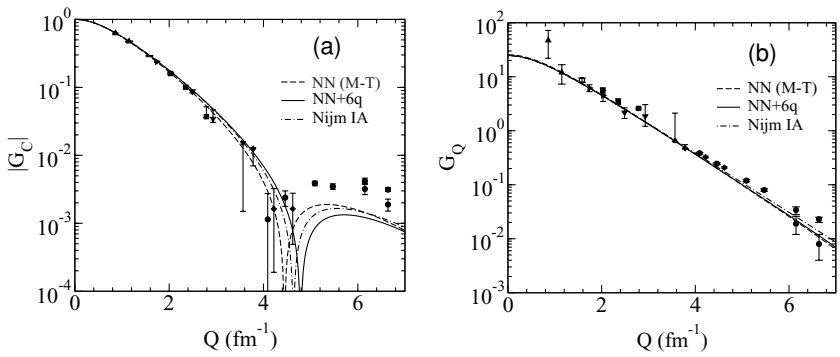

FIG. 4. The Charge G_C (a) and quadrupole G_Q (b) form factors of the deuteron in comparison to the experimental data [61]. Dashed lines correspond to the impulse approximation (IA) for the Moscow-Tuebingen potential model; solid lines correspond to the sum of the IA and the bare dibaryon contribution (the transitions in quark configurations $s^6 \to s^6$ and $s^6 \to s^4p^2$, s^2p^4, $p6$ are taken into account). Dash-dotted lines denote the IA for the Nijmegen93 potential model [62].

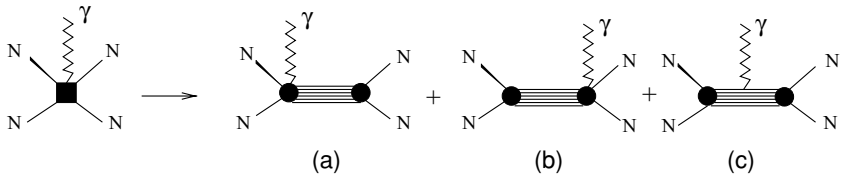

FIG. 5. Schematic representation of the new electromagnetic currents induced by intermediate dibaryon generation.

three-dimensional operator

$$V_{Nq\gamma} = \frac{ieg_s^2}{2m_q}\sum_{i=1}^{3}\sum_{j=4}^{6}\epsilon^{(\lambda)*} \times\left\{v_s\left(\mathbf{k}_j^2\right)\left(\frac{\hat{\mathbf{q}}\,\mathbf{k}_i}{m_q}[\boldsymbol{\sigma}_i\times\hat{\mathbf{q}}]-\frac{[\boldsymbol{\sigma}_i\times\mathbf{k}_i]}{m_q}\right) + v_s\left(\mathbf{k}_i^2\right)\left(-\frac{\hat{\mathbf{q}}\,\mathbf{k}_j}{m_q}[\boldsymbol{\sigma}_j\times\hat{\mathbf{q}}]-\frac{[\boldsymbol{\sigma}_j\times\mathbf{k}_j]}{m_q}\right)\right\} \quad (22)$$

defined for nonrelativistic quark wave functions of the CQM. This operator describes the transition from the NN channel to the $6q$ bag with emission of a $M1$ γ quantum, that is, a "contact" $NN \to \mathrm{DB} + \gamma$ interaction, schematically shown in Fig. 5(a).

Now we can calculate the effective contact vertex $NN \Leftrightarrow NN\gamma$ [see Fig. 5(a)] on the basis of the quark operator $V_{Nq\gamma}$ in terms of the quark-microscopic version of the DB model. Recall that in our model the diagrams in Fig. 7 taken without electromagnetic insertions are simply the pairwise qq interaction:

$$V_{Nq} = g_s^2\sum_{i=1}^{3}\sum_{i=4}^{6}\left[v_s\left(\mathbf{k}_i^2\right)+v_s\left(\mathbf{k}_j^2\right)\right], \quad (23)$$

which describes the transition from the NN- to the $6q$-bag channel (see Fig. 2). This observation points toward the proper solution of the problem of contact $NN \Leftrightarrow NN\gamma$ interaction in our approach. (Further on we use the notation "$NqN\gamma$" for brevity.) Namely, we calculate the nonlocal $NqN\gamma$ interaction operator in the NN Hilbert space $V_{NqN\gamma}(r,r')$ by the same way as the nonlocal NqN interaction operator $V_{NqN}(r,r')$ in Eqs. (4)–(7).

We obtain finally (see Appendix B) the $NqN\gamma$ (contact) term searched for [as the sum of two graphs, Figs. 5(a) and 5(b)]:

$$V^{(\lambda)}_{NqN\gamma}(\mathbf{q};r,r') = \frac{eZ}{2M_N}\left\{i\left[\frac{\boldsymbol{\sigma}_p+\boldsymbol{\sigma}_n}{2}\times\mathbf{q}\right]\epsilon^{(\lambda)*}G_M^S(q^2) + i\left[\frac{\boldsymbol{\sigma}_p-\boldsymbol{\sigma}_n}{2}\times\mathbf{q}\right]\epsilon^{(\lambda)*}G_M^V(q^2)\right\} \times\left\{\frac{1}{q}j_1(qr/2)\frac{d\varphi_{2S}(r)}{dr}\frac{\lambda(E')}{2M_N}\varphi_{2S}(r') + \varphi_{2S}(r)\frac{\lambda(E)}{2M_N}\frac{1}{q}j_1(qr'/2)\frac{d\varphi_{2S}(r')}{dr'}\right\}, \quad (24)$$

where $G_M^S(0)=\mu_p+\mu_n$ and $G_M^V(0)=\mu_p-\mu_n$. [The origin of the nucleon form factors G_M^S and G^V in the quark-model results of Eq. (24) type is discussed in Appendix C.] Our basic expression for the transition dibaryon current still does not take into account possible effects that impact the predictions of our model (namely, relativistic effects and quark boost contributions, which should be essential at $Q^2 \sim 1$ GeV$^2/c^2$ [6], and other contact terms with inclusion of pseudo-scalar and vector-meson exchanges [6,12] etc.). To account effectively for all of these effects we renormalize our contact $NN \Leftrightarrow NN\gamma$ vertex using a renormalization factor Z in Eq. (24). It is felt that the value $Z \approx 1 \pm 0.3$ is reasonable since a precision of 10–30% is typical for standard quark-model evaluations of the hadron magnetic moments. We show in the following that when choosing a reasonable value for the only free constant $Z = 0.7$ the contact term given in Eq. (24) leads to a considerable improvement in the description of the isoscalar magnetic properties of the deuteron.

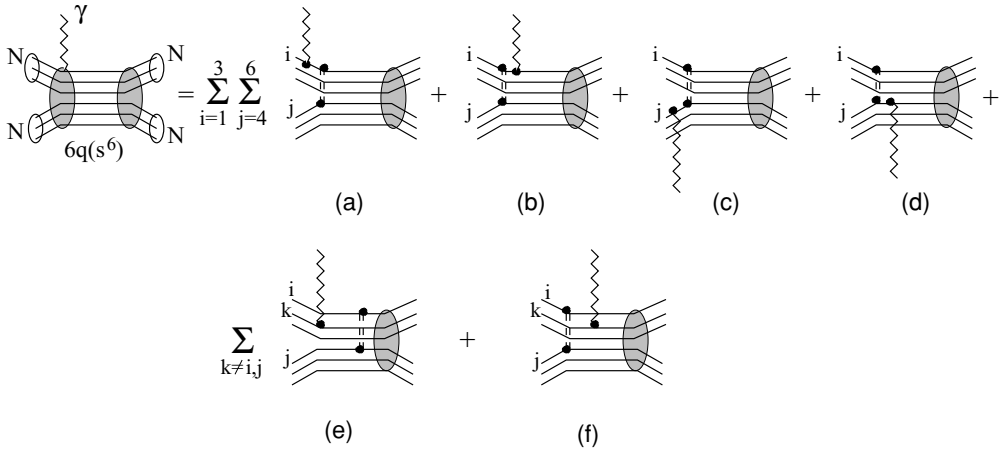

FIG. 6. The diagram series illustrating the contact $V_{Nq\gamma}$ terms contributing to the "nondiagonal" current.

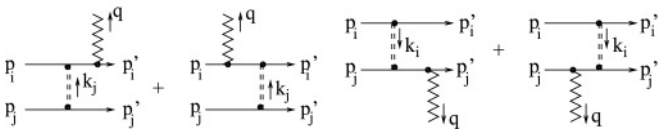

FIG. 7. The part of diagrams shown in Fig. 6 contributing to the nondiagonal dibaryon current with explicit notation of the kinematic variables. The double-dashed line denotes the scalar exchange.

One can get a general expression for the electromagnetic current in the NN system, and also in the deuteron, starting with the quark current [Eq. (20)], which has already been used for finding the contact $NqN\gamma$ vertex (24). When the total deuteron wave function in the Fock-column form [Eq. (10)] is considered, the diagonal matrix element of the quark current [Eq. (20)] can be represented as

$$\begin{aligned}\langle d|\sum_{i=1}^{6} j_i^{\mu}(q)\varepsilon_{\mu}^{(\lambda)}(q)|d\rangle &= \cos^2\theta_{Nq}\langle d(NN)|J_N^{\mu}\varepsilon_{\mu}^{(\lambda)} + V_{NqN\gamma}^{(\lambda)}|d(NN)\rangle \\ &+ \sin^2\theta_{Nq}\langle \mathrm{DB}|\sum_{i=1}^{6} j_i^{\mu}\varepsilon_{\mu}^{(\lambda)}|\mathrm{DB}\rangle \\ &+ 2\cos\theta_{Nq}\sin\theta_{Nq}\langle d(NN)|\sum_{i=1}^{6} j_i^{\mu}\varepsilon_{\mu}^{(\lambda)}|\mathrm{DB}\rangle. \quad (25)\end{aligned}$$

The last two terms in Eq. (25) are nothing but contributions of the graphs shown in Figs. 6(f) and 6(e), respectively.

It is worth summarizing here our main findings. Within our two-component NN interaction model, the minimal substitution leads basically to two different two-particle currents [in addition to the single-nucleon current J_N^{μ} written in the first term of Eq. (25)]: the transition $NN \to \mathrm{DB}$ contact term as given by Eq. (24) and the standard six-quark bag current given by the second and third terms in Eq. (25).

In the nucleon sector we further replace the quark-model (QM) current of the nucleon $J_{N\mathrm{QM}}^{\mu}$ with the standard representation of J_N^{μ} in terms of the phenomenological form factors given in Appendix C by Eqs. (C1) and (C4). However, the two-body current in the last two terms of Eq. (25) (which gives only a small correction to the single-nucleon current J_N^{μ}) is calculated here on the basis of the CQM (see Appendix C for details).

V. ISOSCALAR $M1$ AND $E2$ TRANSITION AMPLITUDES

The effective electromagnetic operator of the isoscalar current $V_{NqN\gamma}^{(\lambda)}$ derived in the previous section is defined, by construction, in a Hilbert space of the NN component of the whole two-component system. Thus, it should be bracketed between the initial and final states just in the NN channel. So, we look here at the application of this new current operator to the three observables: (i) radiative capture $\vec{n} + p \to d + \vec{\gamma}$ of spin-polarized neutrons by hydrogen; (ii) the deuteron magnetic form factor $B(Q^2)$ in the region of its diffraction minimum; and (iii) the very tiny correction to the magnetic moment of the deuteron.

In the radiative capture process, our main interest lies in the calculation of the circular polarization of γ quanta emitted after capture at thermal energies. This includes both $M1$ and $E2$ isoscalar transitions. We can contrast for this process the "contact" isovector and isoscalar transitions, where the corresponding π-exchange term has a long range and corresponds to the isovector transition whereas the scalar-exchange term relates to the short-range $\sigma-$, 2π- or glueball-exchange between quarks in both nucleons (or to the instanton-induced interaction as well) and corresponds to the isoscalar transition. The π-meson isovector current contributes to the total isovector amplitude for the ${}^1S_0 \to {}^3S_1$ transition, which is generally large, and thus this term does not strongly affect the P_γ value, which is governed just by an interference between isovector $M1$ and isoscalar $M1 + E2$ amplitudes. The main point here is that the single-nucleon isoscalar transition is strongly suppressed owing to orthogonality of the initial and final radial wave functions. In this case, the small isoscalar contribution to P_γ and to an angular asymmetry of the photons can be of crucial importance because of their interference with the large isovector amplitude [14,15,63]. The isoscalar $M1$ current can also be very important for the deuteron magnetic form factor $B(Q^2)$ in the area where the contribution of single-nucleon current almost vanishes. So, this new isoscalar current can affect essentially the behavior of $B(Q^2)$ near its minimum.

To fix uniquely the relative signs of the partial transition amplitudes (and for a meaningful comparison between predictions of different models) we use in all our calculations a common expansion of the photon plane wave into vector spherical harmonics (see, e.g., Refs. [64,65]) and a standard choice [66] for the phase factors of Clebsch-Gordon coefficients and spherical functions. This choice fixes the sign of the $E2$ amplitude uniquely. The problem with the relative sign of the $E2$ amplitude would arise if one calculates the $E2$ and $M1$ amplitudes separately (see, e.g., the detailed discussion of the $E2$ sign problem in Refs. [24,67]).

This general formalism, common for two different electromagnetic processes, has been used in the present work jointly with our new NN-force model to estimate a nonadditive two-body current contribution.

A. General consideration

Let us start here with the single-nucleon current. The expansion of the circularly polarized γ-quanta emission (with $\lambda = \pm 1$) operator into electric and magnetic multipoles takes the form [64,65]

$$\begin{aligned}&\vec{J}_N\,\vec{\epsilon}^{\,(\lambda)*}(\hat{q})e^{-i\vec{q}\,\vec{r}/2} \\ &= \frac{-\lambda}{\sqrt{2}}\sum_{l=1}^{\infty}\sqrt{4\pi(2l+1)}(-i)^l\,\vec{J}_N \\ &\quad\times\left\{j_l(qr/2)\vec{Y}^*_{l,l,\lambda}(\hat{r}) - i\lambda\left[\sqrt{\frac{l+1}{2l+1}}\,j_{l-1}(qr/2)\vec{Y}^*_{l,l-1,\lambda}(\hat{r})\right.\right. \\ &\quad\left.\left.-\sqrt{\frac{l}{2l+1}}\,j_{l+1}(qr/2)\vec{Y}^*_{l,l+1,\lambda}(\hat{r})\right]\right\} \quad (26)\end{aligned}$$

in which we employ for vector spherical harmonics

$$\vec{Y}_{j,l,\lambda}(\hat{r}) = \sum_{\varkappa}[l(\lambda-\varkappa)1\varkappa|j\lambda)Y_{l,\lambda-\varkappa}(\hat{r})\,\vec{\epsilon}^{\,(\varkappa)}(\hat{q})], \quad (27)$$

where $\vec{\epsilon}^{\,(\varkappa)}(\hat{q})$ are the basis vectors of circular polarization,

$$\vec{\epsilon}^{\,(\pm1)}(\hat{q}) = \mp\frac{\hat{x}\pm i\hat{y}}{\sqrt{2}}, \qquad \vec{\epsilon}^{\,(0)}(\hat{q}) = \hat{q}. \quad (28)$$

The vectors (28) are determined in the reference frame $X_0Y_0Z_0$ related to the photon (with the coordinate axis Z_0 directed along the photon momentum $\mathbf{q}$, $\hat{\mathbf{z}}_0 = \hat{\mathbf{q}}$).

At thermal energies of neutrons ($v = 2200$ m/s) one can neglect the electric dipole transition $E1$ as the initial P wave is strongly depressed. In Eq. (26) only the two lowest multipoles, $M1$ and $E2$, remain (the $E2$ contribution should not be small because of the $^3S_1$-$^3D_1$ mixing generated by the strong tensor force). The operator of single-nucleon transverse current

$$e\vec{J}_N^{\,T} = \frac{1}{2m_N}\left\{\frac{e_p+e_n}{2}(-2i\vec{\nabla}^{\,T}) + e[(\mu_p\vec{\sigma}_p+\mu_n\vec{\sigma}_n)\times 2\vec{\nabla}_r]\right\} \quad (29)$$

contains $\vec{\nabla}^{\,T}$, a transverse component of the gradient $\vec{\nabla}$ that operates on the initial np wave function, and a gradient $\vec{\nabla}_r = \frac{1}{2}\vec{\nabla}_{r/2}$ operating only on the photon plane wave $e^{-i\vec{q}\,\vec{r}/2}$. Inserting $e\vec{J}_N^{\,T}$ into Eq. (26) one gets, after some algebra, the following representation for the transition amplitude $np \to d\gamma$ in an arbitrary coordinate frame XYZ:

$$T^{(\lambda')}_{MM'}(\varphi,\theta) = \sum_{\lambda=\pm1}\left[M1^{(\lambda)}_{MM'}\mathcal{D}^{(1)}_{\lambda\lambda'}(\varphi,\theta,0) + E2^{(\lambda)}_{MM'}\mathcal{D}^{(2)}_{\lambda\lambda'}(\varphi,\theta,0)\right]. \quad (30)$$

Here the photon emission angles are given in the reference frame XYZ, where the Z axis is chosen along the polarization of the incident neutron. Then the quantum numbers $MM'\lambda'$ are projections of the initial and final spin of the np system and of the photon total angular momentum l, respectively, onto the quantization axis Z, whereas the photon helicity $\lambda = \pm1$ is defined, as before, in its own reference frame $X_0Y_0Z_0$. In correspondence with this the matrix elements for the $M1$ and $E2$ transitions are calculated for the fixed values $\lambda = \pm1$ of the photon helicity, but in an arbitrary reference frame XYZ in which the initial-state wave functions of np scattering are given as

$$\Psi^{np}_M(\vec{r},\vec{p}_n) = \frac{1}{r}\,{}^1S_0(r,p_n)\frac{\delta_{M,0}}{\sqrt{4\pi}}\sum_{\lambda_p,\lambda_n}\left(\tfrac{1}{2}\lambda_p\tfrac{1}{2}\lambda_n|00\right)\chi_{\lambda_p}\chi_{\lambda_n} + \frac{1}{r}\,{}^3S_1(r,p_n)\mathcal{Y}^{01}_{1M}(\hat{r}) + \frac{1}{r}\,{}^3D_1(r,p_n)\mathcal{Y}^{21}_{1M}(\hat{r}) \quad (31)$$

and the final-state wave function reads

$$\Psi^d_{M'}(\vec{r}) = \frac{u(r)}{r}\mathcal{Y}^{01}_{1M}(\hat{r}) + \frac{w(r)}{r}\mathcal{Y}^{21}_{1M}(\hat{r}), \quad (32)$$

where $\mathcal{Y}^{LS}_{JM}(\hat{r}) = \sum_{M_L,M_S}(LM_LSM_S|JM)Y_{LM_L}(\hat{r})\chi_{SM_S}$. The continuum NN states $^1S_0(r,p_n)$ and $^3S_1(r,p_n)$ are normalized by the respective S-wave scattering lengths

$$^1S_0(r,p_n) \to r-a_t, \quad {}^3S_1(r,p_n) \to r-a_s, \quad p_n \to 0, \quad (33)$$

whereas the $^3D_1(r,p_n)$-wave normalization is fixed by the $^3S_1$-$^3D_1$ tensor mixing in the initial state.

After elementary but lengthy calculations, one gets the following formulas for the matrix elements in the right-hand side of Eq. (30):

$$M1^{(\lambda)}_{MM'} = \int d^3r\,\Psi^{d*}_{M'}(\vec{r})\frac{ieq}{2m_N}\lambda\left\{(\mu_n-\mu_p)j_0(qr/2)\,\vec{\epsilon}^{\,(\lambda)*}\times\frac{\vec{\sigma}_p-\vec{\sigma}_n}{2} + (\mu_n+\mu_p)\left[j_0(qr/2)\,\vec{\epsilon}^{\,(\lambda)*}\frac{\vec{\sigma}_p+\vec{\sigma}_n}{2} - \sqrt{\frac{1}{2}}j_2(qr/2)\sqrt{4\pi}\,\vec{Y}^*_{1,2,\lambda}(\hat{r})\frac{\vec{\sigma}_p+\vec{\sigma}_n}{2}\right] + \frac{1}{2}(j_0(qr/2)+j_2(qr/2))\,\vec{\epsilon}^{\,(\lambda)*}\frac{1}{2}\vec{L}\right\}\Psi^{np}_M(\vec{r},\vec{p}_n). \quad (34)$$

The first term in the curly braces corresponds to the isovector $M1$ transition $^1S_0(NN) \to d(^3S_1)$; the remaining two terms describe the isoscalar transitions in the coupled $^3S_1$-$^3D_1$ channels generated by the spin-dependent and convection currents, respectively. In contrast to this, the $E2$ amplitude is purely isoscalar, although it consists of two terms, convection (first) and spin-dependent (second), similarly to the $M1$ amplitude:

$$E2^{(\lambda)}_{MM'} = \int d^3r\,\Psi^{d*}_{M'}(\vec{r})\frac{ieq}{2m_N}\times\left\{\frac{\lambda}{2}[j_0(qr/2)+j_2(qr/2)]\frac{\vec{\epsilon}^{\,(\lambda)*}\vec{L}}{2} - \sqrt{\frac{5}{2}}(\mu_n+\mu_p)j_2(qr/2)\sqrt{4\pi}\,\vec{Y}^*_{2,2,\lambda}(\hat{r})\frac{\vec{\sigma}_p+\vec{\sigma}_n}{2}\right\}\times\Psi^{np}_M(\vec{r},\vec{p}_n). \quad (35)$$

The total $np \to d\gamma$ reaction cross section for unpolarized neutrons can be expressed through the respective amplitudes (34) and (35) in the following way:

$$\sigma^{\rm tot}_{\rm unpol} = \frac{m_n}{p_n}\alpha|\vec{q}|\frac{\vec{q}^{\,2}}{4m_N^2}\frac{1}{3}\sum_{MM'}\sum_{\lambda=\pm1}4\pi\left[\left|M1^{(\lambda)}_{MM',I=1}\right|^2 + \left|M1^{(\lambda)}_{MM',I=0}\right|^2 + \left|E2^{(\lambda)}_{MM'}\right|^2\right]. \quad (36)$$

For the further calculations one can use the well-known properties of the Wigner $\mathcal{D}$ functions, which give the angular behavior of the interference term between $M1$ and $E2$ amplitudes. For example, in radiative capture of spin-polarized neutrons by spin-polarized protons, $\vec{n}+\vec{p} \to d+\gamma$, the angular anisotropy for emission of γ quanta with respect to the spin polarization axis of the initial nucleons can be described.

Let us consider now the asymmetry in circular polarization of γ quanta on the basis of Eqs. (30) and (34)–(36), as measured in the experiment of Ref. [1]. The differential cross section for circularly polarized γ-quanta emission in the forward direction (i.e., along the spin polarization λ_n of

the incident neutron) can be written in terms of the helicity amplitudes (34) and (35):

$$\sigma_\lambda(\lambda_n) = \frac{m_n}{p_n}\alpha|\vec{q}|\frac{\vec{q}^{\,2}}{4m_N^2}\frac{1}{2}\sum_{\lambda_p}\sum_{M'} \times \left|\sum_M \left(\tfrac{1}{2}\lambda_p\tfrac{1}{2}\lambda_n|00\right)M1^{(\lambda)}_{MM',I=1} + \left(\tfrac{1}{2}\lambda_p\tfrac{1}{2}\lambda_n|1M\right)\left[M1^{(\lambda)}_{MM',I=0} + E2^{(\lambda)}_{MM'}\right]\right|^2. \quad (37)$$

For sake of brevity, the differential cross section $d\sigma(\lambda_n, \theta = 0)/d\Omega$ for γ-quanta emission at zero angle with respect to the neutron polarization vector for the case when the neutron spin projection onto the quantization axis equals λ_n is denoted as $\sigma_\lambda(\lambda_n)$. In Eq. (37) we have omitted the Wigner $\mathcal{D}$ functions depicted in Eq. (30) because the respective sums over λ' are reduced, at $\theta = 0$, to the trivial factor 1.

The differential cross section $d\sigma(\lambda_n, \lambda_p; \theta)/d\Omega$ for the photon emission into an arbitrary angle θ can be found using the simple transformation of Eq. (37) by replacing the sum $\frac{1}{2}\sum_{\lambda_p}$ by $\sum_{\lambda=\pm1}$ and by replacing the Wigner $\mathcal{D}$ functions on the right-hand side of Eq. (37).

B. The $\vec{n} + p \to d + \vec{\gamma}$ reaction

Using the general formulas (36) and (37) for the helicity-dependent cross sections one can find the circular polarization $P_\gamma(\lambda_n)$ and angular anisotropy η for the fixed initial values of λ_n (or λ_n, λ_p):

$$P_\gamma(\lambda_n) = \frac{\sigma_{\lambda=1}(\lambda_n) - \sigma_{\lambda=-1}(\lambda_n)}{\sigma_{\text{unpol}}} = \frac{\sum_{\lambda=\pm1}\lambda\sigma_\lambda(\lambda_n)}{\frac{1}{2}\sum_{\lambda_n}\sum_{\lambda=\pm1}\sigma_\lambda(\lambda_n)}, \quad (38)$$

$$\eta(\lambda_n, \lambda_p) = \frac{d\sigma\left(\lambda_n, \lambda_p, \theta = \frac{\pi}{2}\right)/d\Omega - d\sigma(\lambda_n, \lambda_p, \theta = 0)/d\Omega}{d\sigma\left(\lambda_n, \lambda_p, \theta = \frac{\pi}{2}\right)/d\Omega + d\sigma(\lambda_n, \lambda_p, \theta = 0)/d\Omega}. \quad (39)$$

The $M1$ and $E2$ amplitudes that contribute to the cross sections (36) and (37) are given in Appendix D in their exact form. It is important to stress that the dependence of the $M1$ and $E2$ transition matrix elements upon the momentum transfer q in Eqs. (D1)–(D6) is rather weak at low energies and becomes quite significant only for *ed* scattering in the region of moderate and high momenta transfer (see the following). This means that when applying formulas (D1)–(D6) to the $np \to d\gamma$ cross section at thermal energies the integrals I_2 can be neglected and $j_0(qr/2)$ in the integrand of I_0 can be replaced by unity.

As a result, eventually the expression for P_γ can be presented via more simple "reduced" matrix elements

$$\begin{aligned} M1_{I=1} &= (\mu_p - \mu_n)I_0\left(u, {}^1S_0\right), \\ M1_{I=0} &= (\mu_p + \mu_n)\left[I_0\left(u, {}^3S_1\right) - \tfrac{1}{2}I_0\left(w, {}^3D_1\right)\right] \\ &\quad + \tfrac{3}{8}I_0\left(w, {}^3D_1\right), \\ E2_{I=0} &= \tfrac{3}{8}I_0\left(w, {}^3D_1\right), \end{aligned} \quad (40)$$

with $I_0(f, Z) = \int_0^\infty f(r)Z(r, p_n)\,dr$, where $Z(r, p_n)$ can be any of the scattering wave functions in the ${}^1S_0, {}^3S_1$, or ${}^3D_1$ channels. Thus we get eventually

$$P_\gamma(\lambda_n) = (-1)^{1/2+\lambda_n}P_\gamma, \quad P_\gamma = 2\text{Re}\left\{\frac{M1_0}{M1_1} + \frac{E2_0}{M1_1}\right\}, \quad (41)$$

in which the factor $(-1)^{1/2+\lambda_n}$ in front of P_γ reflects only that dependence on λ_n, which is deduced from the Clebsch-Gordon coefficient $(\frac{1}{2}\lambda_p\frac{1}{2}\lambda_n|00) = (-1)^{1/2+\lambda_n}\sqrt{\frac{1}{2}}$ in the first term of Eq. (37). Moreover, since in the limit $p_n \to 0$ all ratios of the matrix elements in Eqs. (D1) and (40) become real, the symbol Re can be omitted here.

Quite similar considerations regarding the angular anisotropy η yield a formula quadratic with respect to the matrix elements in Eqs. (40) and bilinear on spin-polarizations of the neutron and the proton [14,15].

In the literature there are calculations for P_γ with the Reid soft core (RSC) potential, but the published results [24] do not include any details and any patterns owing to the interference of various $M1$ and $E2$ terms. Therefore, we also perform a parallel calculation for the value of P_γ with the well-known Reid NN potential (version Reid 93 [58]). Thus, the detailed comparison for all partial contributions between our model and the conventional RSC potential model sheds light on the delicate balance of different isoscalar current components to the total value of P_γ.

C. Deuteron magnetic form factor

Usually the deuteron magnetic form factor includes a contribution of the transverse current [Eq. (29)] as a whole without explicit separation into $M1$ and $E2$ multipoles. However, in the calculations of the deuteron magnetic form factor we still can employ the helicity amplitudes (34) and (35) derived here by summing and substituting the deuteron wave functions u and w instead of the wave functions ${}^3S_1$ and ${}^3D_1$ in the continuum. In this substitution the isovector part [the first term of Eq. (34)] automatically vanishes while in the isoscalar part the electric charge e (in the convection current term) and the magnetic moment $(\mu_p + \mu_n)$ in the spin-dependent term are replaced with their respective isoscalar counterparts, namely the isoscalar electric and magnetic form factors of the nucleon

$$\begin{aligned} G_E^s(q^2) &= G_E^p(q^2) + G_E^n(q^2), \\ G_M^s(q^2) &= G_M^p(q^2) + G_M^n(q^2), \\ q^2 &= q_0^2 - \vec{q}^{\,2}. \end{aligned} \quad (42)$$

As a result, the sum of $M1$ and $E2$ contributions [see Eqs. (D2)–(D5) in Appendix D] is transformed into the well-known formula for the deuteron magnetic form factor

$$G_M^d(q^2) = \sqrt{\frac{2}{3}}\frac{\sqrt{-q^2}}{2m_N}\left\{\frac{3}{4}G_E^s(q^2)\int_0^\infty w^2(r)[j_0(qr/2) + j_2(qr/2)]dr + G_M^s(q^2)\right.$$

$$\times \int_0^\infty \left[\left(u^2(r) - \frac{1}{2} w^2(r) \right) j_0(qr/2) + \frac{w(r)}{\sqrt{2}} \left(u(r) + \frac{w(r)}{\sqrt{2}} \right) j_2(qr/2) \right] dr \Bigg\}, \quad (43)$$

where the factor $\sqrt{2/3}$ accounts for the averaging of the amplitude squared over the spin projections. This gives the standard normalization of the deuteron magnetic form factor, which leads to the conventional expression for the deuteron structure functions A and B:

$$A(q^2) = \left[G^d_{C0}(q^2)\right]^2 + \left[G^d_{C2}(q^2)\right]^2 + \left[G^d_M(q^2)\right]^2,$$
$$B(q^2) = 2(1+\eta_d)\left[G^d_M(q^2)\right]^2, \quad \eta_d = \frac{-q^2}{4m_d^2}. \quad (44)$$

The cross section for elastic ed scattering is written as

$$\frac{d\sigma_{ed}}{d\Omega} = \frac{\sigma_{\text{Mott}}}{1 + \frac{2E}{m_d} \sin^2 \frac{\theta}{2}} \left\{ A(q^2) + B(q^2) \tan^2 \frac{\theta}{2} \right\}. \quad (45)$$

The expression in the curly braces of Eq. (43) evolves in the limit $Q^2 \to 0$ and it goes to the well-known formula for the deuteron magnetic moment

$$\mu_d(NN) = \mu_p + \mu_n - \frac{3}{2}\left(\mu_p + \mu_n - \frac{1}{2}\right) P_D,$$
$$P_D = \int_0^\infty w^2(r)\, dr. \quad (46)$$

VI. COMPARISON WITH EXPERIMENTAL DATA

When calculating the dibaryon and quark contributions to both physical processes one begins from the general formula (34) for the $M1$ amplitude and modifies its spin-dependent part. The contribution of the contact dibaryon-induced interaction can be found by replacing the isoscalar nucleon spin-current operator in Eq. (34),

$$\frac{ieq}{2m_N} \lambda(\mu_n + \mu_p) j_0(qr/2)\, \vec{\epsilon}^{\,(\lambda)*} \frac{\vec{\sigma}_p + \vec{\sigma}_n}{2}, \quad (47)$$

with the respective spin-dependent operator for the dibaryon contact term [Eq. (24)]. Consequently, in the left bra-vector of the matrix element [Eq. (34)] one needs to use the deuteron wave function Ψ^d instead of Ψ^{np}. Moreover, one can ignore in this case the energy dependence of the nonlocal potential $V_{NqN}(r', r; E)$ in Eq. (1) and substitute $E = 0$ there instead of the real energy ε_T of thermal neutrons or the bound-state energy of the deuteron, E_d, since the scale of the $\lambda(E)$ factor in Eqs. (1) and (2) is much larger and of the order $E_0 \sim 1$ GeV. With these reasonable approximations one calculates first the isoscalar current contribution to the deuteron magnetic moment.

A. The deuteron magnetic moment and the deuteron form factor

In our model the deuteron magnetic form factor takes the form

$$G^d_M(q^2) = \sqrt{\frac{2}{3}} \frac{\sqrt{-q^2}}{2M_N} \big[\cos^2\theta_{Nq} G^d_{M(NN)}(q^2) + \cos^2\theta_{Nq}\, \mu_{NqN} F_{NqN}(q^2) + \sin^2\theta_{Nq}\, \mu_{s^6} F_{s^6}(q^2) + 2\cos\theta_{Nq} \sin\theta_{Nq}\, \mu_{s^6-s^4p^2} F_{s^6-s^4p^2}(q^2) \big], \quad (48)$$

where the first term in the brackets represents the nucleonic current contribution and the second one corresponds to the isoscalar component of the contact $NN \Leftrightarrow NN\gamma$ vertex [Eq. (24)]:

$$\mu_{NqN} F_{NqN}(q^2) = G^S_M(q^2)\, 2Z \int_0^\infty \int_0^\infty dr dr' u(r) u(r') \times \varphi_{2S}(r) \frac{\lambda(0)}{2M_N} \frac{1}{q} j_1(qr'/2) \frac{d\varphi_{2S}(r')}{dr'}. \quad (49)$$

Here, $F_{NqN}(0) = 1$ by definition and thus the value μ_{NqN} is equal to that of the right-hand-side integral at $q = 0$. The third and fourth terms in Eq. (48) represent the diagonal and nondiagonal contributions of the $6q$ core of the dibaryon (i.e., the bare dibaryon contribution). As is evident from Eq. (C6) of Appendix C the last term in Eq. (25) vanishes at $q = 0$ and thus does not contribute to the deuteron magnetic moment; accountting for the second term in Eq. (25) results only in a minor renormalization of the deuteron magnetic moment (46). As a result, the dressed bag gives a real contribution to the deuteron magnetic moment only from the contact $NN \Leftrightarrow NN\gamma$ vertex [Eq. (24)], and this contribution is equal to

$$\Delta\mu_d^{\text{DB}} = \cos^2\theta_{Nq}\, \mu_{NqN}. \quad (50)$$

In all the present calculations for the deuteron magnetic moment and the structure function $B(Q^2)$, the published parameters [Eqs. (19)] of the MT NN model have been employed. These parameters allow fitting of the NN phase shifts over the very large energy interval (0–1000 MeV). The mixing parameter θ_{Nq} can also be calculated with the MT model, amounting to

$$\sin\theta_{Nq} = -0.13886. \quad (51)$$

The first term in Eq. (48) is calculated with Eq. (46), whereas the third and fourth terms are calculated via Eqs. (C5) and (C6) of Appendix C. The sum of these three terms to the deuteron magnetic moment amounts to

$$\mu_d = \cos^2\theta_{Nq}\, \mu_d(NN) + \sin^2\theta_{Nq}\, \mu_d(6q) = 0.8489\,\text{n.m.}, \quad (52)$$

as shown in Table I. From the difference of this theoretical prediction to the respective experimental value $\mu_d^{\text{exp}} = 0.8574$ n.m. one can find an admissible value for the contact-term contribution [Eq. (50)], which amounts in our case to be value $\Delta\mu_d^{\text{DB}} \sim 0.01$ n.m. The second term in Eq. (48) is calculated with Eqs. (49) and (50) and we employ the fixed values from Eqs. (19) and (51) and $Z = 1$ in Eq. (24). Thus, in this calculation for $\Delta\mu_d^{\text{DB}}$ we do not use any free

parameters and reach a value

$$\Delta\mu_d^{\mathrm{DB}} = 0.0159\,\mathrm{n.m.}, \tag{53}$$

which is in very reasonable agreement with the preceding limitation. The resulting value for the deuteron magnetic moment $\mu_d^{\mathrm{theor}} = 0.8648$ n.m. overshoots the respective experimental value a little, but the remaining disagreement $\Delta\mu = 0.0074$ n.m. has decreased considerably.

This value for μ_d^{theor} can be compared to the result of a recent calculation [10] within the framework of the Bonn OBEPQ model with leading-order relativistic corrections (RC): $\mu_d(\text{Bonn OBEPQ [10]+RC}) = 0.8875$ n.m. This notable overestimation of the μ_d originated mainly from the π- and ρ-MEC contributions points clearly to some abundance of high-momentum components in the deuteron wave function because of the enhancement of the cutoff parameters $\Lambda_{\pi NN}$, $\Lambda_{\rho NN}$, etc.

To reproduce exactly the deuteron magnetic moment within our approach, we fix the value of the renormalization constant Z to $Z = 0.7$. We consider the accurate experimental value for the deuteron magnetic moment to give a stringent test for any new isoscalar current contribution. With the fixed renormalization constant $Z = 0.7$ we calculate further the deuteron magnetic form factor and the circular polarization P_γ. Without any other adjustments we follow this strategy to obtain a parameter-free estimate for the latter observables.

Behavior of the structure function $B(Q^2)$ near its minimum at $Q^2 \simeq 2\ \mathrm{GeV}^2/c^2$ corresponding to $Q \simeq 7\ \mathrm{fm}^{-1}$ gives a very stringent test for the new baryon-induced current. The position of the minimum depends crucially upon nonadditive two-body contributions. In Fig. 8(b) we display the results of our calculation for $B(Q^2)$ based on Eq. (48) and we compare them to the experimental data [3–5]. The dashed curve in Fig. 8(b) represents the single-nucleon current contribution, which is described by the term proportional to $G^d_{M(NN)}(q^2)$. The position of the minimum for this single-nucleon term appears noticeably shifted toward lower Q^2 values as compared to the experimental data [3–5]. Adding the conventional quark contribution [dotted line in Fig. 8(b)] reduces this discrepancy owing to the positive sign of the s^6-bag contribution, which is approximately compensated by the negative-sign interference term between the nucleon and the bag contributions. It is evident however from this consideration that one needs some positive contribution to reproduce the correct position of the minimum.

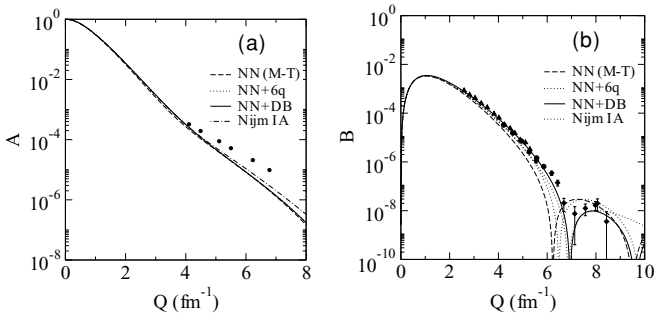

FIG. 8. The structure functions $A(Q)$ (a) and $B(Q)$ (b) of elastic e-d scattering. Dashed lines denote the IA for the Moscow-Tuebingen potential model [23]. Dotted lines show the sum of IA and the diagonal ($s^6 \to s^6$) and nondiagonal ($s^6 \to s^4p^2$, s^2p^4, p^6) bare $6q$ contributions. For comparison the IA for the Nijmegen93 potential [62] is shown (dash-dotted). Solid lines show the total contribution of the IA, the bare dibaryon, and the DB contact term. The data are from [3–5].

In the model developed here, the contact term, which is tightly related to the intermediate dibaryon production, has just the necessary properties. Adding the contribution of the DB contact term [Eq. (49)] in line with Eq. (48) results immediately in a very good description for the deuteron magnetic form factor $B(Q^2)$, as shown by the solid line in Fig. 8(b).

Thus, a rather minor renormalization of the DB contact term by a factor of 0.7 makes it possible to describe quantitatively both the deuteron magnetic moment μ and the behavior of $B(Q^2)$ in the large momentum transfer region $Q^2 \lesssim 2.5\ \mathrm{GeV}^2/c^2$. Moreover, with this fixed value of Z the calculation of the circular polarization P_γ will be fully parameter free.

B. The circular polarization of photons in the reaction $\vec{n} + p \to d + \vec{\gamma}$

The contribution of the dibaryon current to the isoscalar $M1$ transition ${}^3S_1(NN) \to {}^3S_1(d)$ is calculated now in the same way. When the spin-dependent operator [Eq. (47)] in the matrix element [Eq. (34)] is replaced by the contact term [Eq. (24)] the $M1$ transition amplitude for the circularly polarized γ-quanta emission is obtained as

$$\begin{aligned}\Delta M1^{(\lambda)}_{MM'} = Z \int d^3r' \int d^3r\, \Psi^d_{M'}(\vec{r}\,')\frac{e}{2M_N} i\left[\frac{\boldsymbol{\sigma}_p + \boldsymbol{\sigma}_n}{2} \times \mathbf{q}\right] \\ \times \boldsymbol{\epsilon}^{(\lambda)*} G^S_M(q^2)\left\{\frac{1}{q} j_1(qr/2)\frac{d\varphi_{2S}(r)}{dr}\frac{\lambda(E_d)}{2M_N}\right. \\ \left. \times\ \varphi_{2S}(r') + \varphi_{2S}(r)\frac{\lambda(\varepsilon_T)}{2M_N}\frac{1}{q} j_1(qr'/2)\frac{d\varphi_{2S}(r')}{dr'}\right\} \\ \times \Psi^{np}_M(\vec{r}, \vec{p}_n).\end{aligned} \tag{54}$$

When calculating P_γ this amplitude must be added to the single-nucleon current terms [Eqs. (40)] using the same renormalization constant $Z = 0.7$. Similarly to the single-nucleon current, the integral (54) is calculated straightforwardly by replacement of $j_1(qr/2)/q \to r/6$ by $q = E_d$. Also we substitute $E = 0$ instead of $E = \varepsilon_T$ and $E = E_d$ in the $\lambda(E)$ function in Eq. (2). After this we get for the dibaryon-induced current contribution an expression analogous to Eq. (D2) with the respective "reduced" dibaryon matrix elements. The amplitude [Eq. (54)] found by this way together with the single-nucleon matrix elements [Eqs. (40)] should be included to the final expression for P_γ:

$$P_\gamma^{\mathrm{tot}} = 2\mathrm{Re}\left\{\frac{M1_0}{M1_1} + \frac{\Delta M1}{M1_1} + \frac{E2_0}{M1_1}\right\}, \tag{55}$$

where the dibaryon-induced current contribution is

$$P_\gamma(\mathrm{DB}) = 2\mathrm{Re}\left\{\frac{\Delta M1}{M1_1}\right\}. \tag{56}$$

TABLE II. Circular polarization P_γ of γ quanta in the $\vec{n} + p \to d + \vec{\gamma}$ reaction.

Model	$P_\gamma(M1)$ $\times 10^{-3}$	$P_\gamma(E2)$ $\times 10^{-3}$	$P_\gamma(NN)$ $\times 10^{-3}$	P_γ(DB) $\times 10^{-3}$	$P_\gamma^{\rm tot} \times 10^{-3}$
Reid 93	−1.761	0.699	−1.062	0.	−1.062
M-T	−1.791	0.657	−1.134	−0.261	−1.395
Exp. [1]					-1.5 ± 0.3

The results of the numerical calculations within our model are presented in Table II together with a parallel calculation for P_γ with the conventional RSC NN-potential model in its modern version RSC93 [58]. Evidently the fully parameter free prediction of our dibaryon model for P_γ is for the first time in very good agreement with the respective experimental result.

VII. SHORT DISCUSSION AND CONCLUSION

In this paper we developed a model for the new electromagnetic current in the deuteron and in the NN system in general. The new currents are based on the picture of a short-range NN interaction via an intermediate dibaryon generation. The dibaryon represents a new degree of freedom and according to a general principle of quantum theory this must inevitably lead to the respective new current(s). By applying the general recipe of minimal substitution to the Hamiltonian of the dibaryon model to derive the new current one gets automatically two different contributions: diagonal and transitional ones. The diagonal current is associated mainly with the quark degrees of freedom, and thus it is proportional to the (small) weight of the dibaryon component in the deuteron. The transitional current leads to a larger contribution to the deuteron electromagnetic properties, and likely also to NN electromagnetic observables, especially of an isoscalar nature. We studied three such electromagnetic characteristics:

(i) the magnetic moment μ_d of the deuteron;
(ii) the magnetic form factor $B(Q^2)$ in the region of its diffraction minimum; and
(iii) the circular polarization P_γ of γ quanta in radiative capture of spin-polarized neutrons by hydrogen.

As for the prediction of the deuteron magnetic moment, the new isoscalar dibaryon current just fills perfectly the small gap that was found earlier ($\Delta\mu \simeq 0.010$ n.m.) between prediction of the dibaryon NN-force model and experimental data (see Table I). With this tiny correction the theoretical deuteron magnetic moment μ_d agrees excellently with its respective experimental value.

In the present study we found that the minimal (gauge) substitution to the dibaryon Hamiltonian gives a strong positive contribution to the $B(Q^2)$ behavior near the minimum region. Moreover, the parameter-free calculation of $B(Q^2)$ in the new model already gives a very reasonable description for the deuteron magnetic form factor $B(Q^2)$. A minor reduction of the dibaryon-γ vertex by a factor 0.7 results in excellent agreement with the data both for μ_d and $B(Q^2)$.

After fixing all parameters of the new model, we calculated the magnitude of the circular polarization of photons in $\vec{n} + p \to d + \gamma$ capture at thermal energy. This fully parameter free calculation gave a result that is in very close agreement with the existing experimental data [1]. It is important to remind the reader that many attempts were undertaken in the past; see, for example, the review of Rho and co-workers [14], where one can find the references to earlier works and a good discussion of all difficulties encountered in theoretical predictions of P_γ. Thus, this longstanding P_γ puzzle seems now to be solved.

It is useful to discuss briefly the comparison between the present model predictions and some other current models, both microscopic and phenomenological ones. Very detailed six-quark microscopic calculations in Ref. [31] have revealed that the quark-exchange currents cannot give any quantitative agreement with deuteron data for either the magnetic or the charge form factors, $B(Q^2)$ and $A(Q^2)$, respectively. Moreover, when calculating the quark-exchange current corrections to the magnetic and quadrupole deuteron moments the authors [31] have found some (although minor) underestimation for μ_d but strong *overestimation* for Q_d. These disagreements with the respective experimental results have demonstrated that the incorporation of a bare six-quark contribution only cannot fill the gap between the impulse approximation (plus the traditional MEC) results and the experiment, at least for the $M1$ and $E2$ isoscalar transitions. However, the dressing procedure for the six-quark bag has been shown in the present work to lead inevitably to new short-range currents. These dibaryon-induced currents should replace the conventional two-body meson-exchange currents at short NN distances when two interacting nucleons are overlapping strongly, in which case their meson clouds will fuse into one common cloud of a dibaryon.

The new dibaryon currents proposed and studied in this paper must also contribute to many other electromagnetic properties that previously could not be explained with the conventional NN models (e.g., the γ-induced polarization of nucleons in the photo-disintegration of the deuteron at low energies, $d(\gamma, \vec{n})p$, and also the electro-disintegration of the deuteron, $d(e, e'p)n$, at high momentum transfer [68]). The particular interest in the new isoscalar current rests in numerous studies of $(e, e'pp)$ and (γ, pp) processes at intermediate energies. It is worth remembering here that the theoretical interpretation of such processes, measured experimentally at various kinematic conditions, failed to explain the accurate experimental findings (see, e.g., Ref. [69]). Very likely these processes include some contribution of two-body isoscalar currents as well.

Simultaneously, any success in such a consistent interpretation of the data will strongly support the underlying dibaryon model for the short-range NN interaction.

ACKNOWLEDGMENTS

The authors wish to thank Professors S. V. Gerasimov and V. E. Lyubovitskij for very fruitful discussions and Drs. M. Kaskulov, V. N. Pomerantsev, and M. A. Shikhalev

for interesting discussions and help in part of the numerical work. This work was partially supported by the Russian Foundation for Basic Research (Grant Nos. 05-02-04000 and 05-02-17407) and the Deutsche Forschungsgemeinschaft (Grant No. 436 RUS 113/790).

APPENDIX A: AVOIDING DOUBLE COUNTING

It is worth adding here some important comments about the large difference between "diagonal" and "nondiagonal" (transition) currents in the NN system. It is important that similar consideration of the t-channel two-body currents in the NN system (with replacement of the quarks by nucleons in Fig. 7) within the framework of a traditional NN model does not lead to new currents because the scalar exchange in the t channel is already included somehow into the NN wave function Ψ_{NN}, and thus the one-nucleon current matrix element $\langle\Psi_{NN}|J^{\mu}_{N}|\Psi_{NN}\rangle$ also includes (among others) the diagrams shown in Fig. 7.

In contrast to this (one-channel) problem, we are dealing here with a two- (or more) channel problem and our nondiagonal current operator $V_{Nq\gamma}$ given in Eq. (22) describes an electromagnetic-induced transition between two different channels, that is, between the proper NN and dressed bag components. In such transitions there is a strong rearrangement of the spin-isospin structure of the total six-quark wave function, and thus this transition between two components is associated with the real current of magnetic type, which corresponds to the quark spin (isospin) flip. This can be illustrated clearly by considering a transition $|s^4p^2[42]_X\rangle \to |s^6[6]_X\rangle$ even with the same value of the total spin S (and isospin T) in the left (bra) and right (ket) vectors in the current matrix element: $\langle s^6[6]_X, ST|V_{Nq\gamma}|s^4p^2[42]_X, ST\rangle$. Recall also that the configuration s^6 in our model is fully absent in the initial and final NN states because of the orthogonality condition (12) and the projector appearing in the NN channel.

Let us assume that the spin and isospin in the initial (and final) NN channel and in the intermediate dibaryon state have the values $S = 1$ and $T = 0$, which are associated with the spin and isospin Young tableaux for the six-quark system $[42]_S$ and $[3^2]_T$, respectively. As a result, we get the following transition matrix element:

$$\langle s^6[6]_X[42]_S[3^2]_T([f'_{ST}]),\\ [2^3]_C|V_{Nq\gamma}|s^4p^2[42]_X[42]_S[3^2]_T([f_{ST}]),\quad [2^3]_C\rangle. \tag{A1}$$

It is important to stress here that $[f'_{ST}] \neq [f_{ST}]$; that is, the spin-isospin structure in bra and ket states are different, because the Pauli principle severely restricts the form of the spin-isospin tableau $[f'_{ST}]$ on the left-hand side state, reducing it to a single allowable state $[42]_S \circ [3^2]_T \to [f'_{ST}] = [3^2]_{ST}$. In contrast, on the right-hand side state, any spin-isospin Young tableau $[42]_S \circ [3^2]_T \to [f_{ST}] = [51]_{ST} + [41^2]_{ST} + [3^2]_{ST} + [321]_{ST} + [2^21^2]_{ST}$ is permissible (see, e.g., Refs. [50,70]).

Therefore even the static magnetic moments for left and right functions must be different. It is worth remembering here that just the spin-isospin Young tableau $[f]_{ST}$ determines fully the nucleon magnetic moment μ_N at $S = 1/2$ and $T = 1/2$, and the correct value μ_N for both the proton and the neutron can be obtained only for the symmetric ST state $[3]_{ST}$ satisfying the Pauli exclusion principle. Hence, in the transitions (A1) we have real currents describing the spin-isospin flip in the $NN \to$ DB transition, and thus, the current operator $V_{Nq\gamma}$ makes a nontrivial (two-body) contribution to the total current in the two-channel system $NN +$ DB.

APPENDIX B: DERIVATION OF THE CONTACT $NN \Leftrightarrow NN\gamma$ TERM

When deriving Eq. (24) we start from Eq. (4) and substitute the vertex $Nq\gamma$ (22) in one matrix element of the $s^4p^2 \to s^6$ transition $\langle s^4p^2\{f\}|V_{Nq}|s^6[6]_X\rangle$ on the right-hand side of Eq. (4). This gives

$$\begin{aligned} V_{NqN\gamma} \simeq \sum_{ff'}[&\langle NN|s^4p^2\{f\}\rangle\,\langle s^4p^2\{f\}|V_{Nq\gamma}|s^6\rangle G_{\rm DB}\\ &\times\langle s^6|V_{Nq}|s^4p^2\{f'\}\rangle\,\langle s^4p^2\{f'\}|NN\rangle\\ &+\langle NN|s^4p^2\{f\}\{\,\rangle s^4p^2\{f\}|V_{Nq}|s^6\rangle G_{\rm DB}\\ &\times\langle s^6|V_{Nq\gamma}|s^4p^2\{f'\}\{\,\rangle s^4p^2\{f'\}|NN\rangle] \end{aligned} \tag{B1}$$

(where nonsignificant details are omitted here). The calculation of this operator is performed with the fractional parentage coefficient technique (see Refs. [50,51,70,71] for details) by factorizing the fixed pair ij of quarks with numbers $i = 3$ and $j = 6$. The space coordinates of this pair depend on proton and neutron c.m. coordinates $\mathbf{r}_p$ and $\mathbf{r}_n$, respectively, and on the relative motion Jacobi coordinates $\boldsymbol{\rho}_{p1}$, $\boldsymbol{\rho}_{p2}$, $\boldsymbol{\rho}_{n1}$, and $\boldsymbol{\rho}_{n2}$, as defined in Eq. (6) and in the following:

$$\begin{aligned} &\mathbf{r}_3 = \mathbf{R} + \mathbf{r}_p - 2\boldsymbol{\rho}_{p2}/3, \quad \mathbf{r}_6 = \mathbf{R} + \mathbf{r}_n - 2\boldsymbol{\rho}_{n2}/3,\\ &\mathbf{R} = \frac{1}{6}\sum_{i=1}^{6}\mathbf{r}_i. \end{aligned} \tag{B2}$$

In the c.m. frame $\mathbf{R} = 0$ and $\mathbf{r}_p = -\mathbf{r}_n = \mathbf{r}/2$. The conjugated momenta $\mathbf{p}_3$ and $\mathbf{p}_6$ read

$$\begin{aligned} \mathbf{p}_3 &= \mathbf{P} + 2(\mathbf{p}_p - \mathbf{p}_n)/3 - \boldsymbol{\pi}_{p2},\\ \mathbf{p}_6 &= \mathbf{P} - 2(\mathbf{p}_p - \mathbf{p}_n)/3 - \boldsymbol{\pi}_{n2}, \end{aligned} \tag{B3}$$

where $\boldsymbol{\pi}_{p2}$ and $\boldsymbol{\pi}_{n2}$ are the relative momenta conjugated to $\boldsymbol{\rho}_{p2}$ and $\boldsymbol{\rho}_{n2}$, respectively, with $\mathbf{P} = \sum_{i=1}^{6}\mathbf{p}_i$.

The calculation of the Fourier transform $\int \frac{d^3p_1}{(2\pi)^3}\ldots\int \frac{d^3p_6}{(2\pi)^3}\exp(i\mathbf{p}_1\mathbf{r}_1 + \ldots + i\mathbf{p}_6\mathbf{r}_6)$ for the matrix elements of operators $V_{Nq\gamma}$ and V_{Nq} on the right-hand side of Eq. (B1) and substitution of the integral $\int \exp[-i(\mathbf{p}_3 + \mathbf{p}_6 - \mathbf{p}'_3 - \mathbf{p}'_6 - \mathbf{q})\mathbf{x}]d\mathbf{x}$ for the δ function $(2\pi)^3\delta^3(\mathbf{p}_3 + \mathbf{p}_6 - \mathbf{p}'_3 - \mathbf{p}'_6 - \mathbf{q})$ lead, after some simple but tedious mathematics, to the following expression for the r-dependent part of the $NN \to$ DB $+ \gamma$ vertex in Eq. (B1):

$$\begin{aligned} \tilde{V}_{Nq\gamma}(q,r) = \frac{e}{2M_N}F_N(\mathbf{q}^2)\,g_s^2\,\langle v\rangle\Big\{&e^{-i\mathbf{q}\mathbf{r}/2}\mu_p\frac{1}{M_N}\nabla_r[\boldsymbol{\epsilon}^{(\lambda)}\\ &\times\boldsymbol{\sigma}_p] - e^{i\mathbf{q}\mathbf{r}/2}\mu_n\frac{1}{M_N}\nabla_r[\boldsymbol{\epsilon}^{(\lambda)}\times\boldsymbol{\sigma}_n]\Big\}\varphi_{2S}(r). \end{aligned} \tag{B4}$$

The terms with factors $\frac{\hat{\mathbf{q}}\,\mathbf{k}_i}{m_q}[\boldsymbol{\sigma}_i \times \hat{\mathbf{q}}]$ on the right-hand side of Eq. (22) cancel after the summation in Eq. (B1). Now the expression (B4) should replace the function $\varphi(r)\varphi_{2S}(r)$ in the separable potential (1) in line with the interpretation of the vertex matrix element in Eq. (7).

In Eq. (B4) we use the standard formulas of CQM for the nucleon form factor,

$$F_N(\mathbf{q}^2) = F_q(q^2)\int |\psi_N(\rho_1, \rho_2))|^2 e^{2i\boldsymbol{\rho}_2\mathbf{q}/3} d^3\rho_1 d^3\rho_2, \quad \text{(B5)}$$

and for the magnetic momentum of the nucleon,

$$\langle N(3q), [21]_s[21]_\tau : [3]_{ST}| \times \sum_{i=1}^{3} \frac{\hat{e}_i \boldsymbol{\sigma}_i}{2m_q} |N(3q), [21]_s[21]_\tau : [3]_{ST}\rangle = \frac{\mu_N \boldsymbol{\sigma}_N}{2M_N}, \quad \text{(B6)}$$

where $N = n, p$, with $\mu_p = 3$ and $\mu_n = -2$. The gradients in Eq. (B4) originate from the proton and neutron momenta $\mathbf{k}_p$ and $\mathbf{k}_n$, which appear in the momentum representation of the vertex (B4) as a result of substitution of Eqs. (B3) for the quark momenta $\mathbf{p}_3$ and $\mathbf{p}_6$. In the coordinate representation, these momenta transform into gradients $-i\nabla_{r_p} = -i\nabla_{r/2}$ and $-i\nabla_{r_n} = i\nabla_{r/2}$, respectively. The nucleon mass M_N in Eq. (B6) is a result of the substitution of M_N for the value $3m_q$ that appears on the right-hand side of Eq. (B1) resulting from CQM algebra.

Making use of the expressions

$$\nabla_r \varphi_{2S}(r) = \hat{\mathbf{r}}\frac{d}{dr}\varphi_{2S}(r),$$
$$e^{\pm i\mathbf{q}\,\mathbf{r}/2} = j_0(qr/2) \pm i\sqrt{4\pi}\, j_1(qr/2) \times \sum_m Y_{1m}(\hat{q}) Y^*_{1m}(\hat{r}) + \ldots, \quad \text{(B7)}$$

and adding the contributions of two graphs (a) and (b) depicted in Fig. 5 we obtain finally Eq. (24) for the $NqN\gamma$ (contact) term.

APPENDIX C: NUCLEON AND DIBARYON ELECTROMAGNETIC MATRIX ELEMENTS

The general formula for the nucleon electromagnetic current

$$eJ^\mu_N = e_N\gamma^\mu F_1^N(q^2) + i\frac{e\mu_N - e_N}{2M_N}\sigma^{\mu\nu}q^\nu F_2^N(q^2),$$
$$e_N = e\left(\frac{1}{2} + \frac{\tau_z}{2}\right) \quad \text{(C1)}$$

can easily be derived after averaging the quark current (20) over the nucleon wave function:

$$eJ^\mu_{N\mathrm{QM}} = \langle N(123)|\sum_{i=1}^{3} j_i^\mu(q)|N(123)\rangle = \left[e_N\gamma^\mu + i\frac{e\mu_{N\mathrm{QM}} - e_N}{2M_N}\sigma^{\mu\nu}q^\nu\right]F_{\mathrm{QM}}(q^2), \quad \text{(C2)}$$

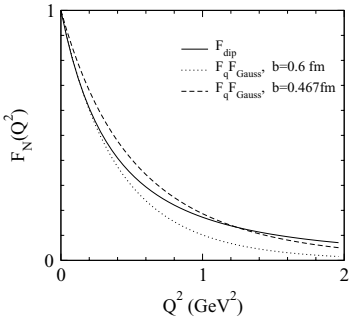

FIG. 9. Comparison of the simple quark-model description for the nucleon magnetic form factor (with different scale values b) with those parametrized through the standard dipole fit.

in which the quark-model predictions

$$\mu_{p\mathrm{QM}} = 3, \quad \mu_{n\mathrm{QM}} = -2,$$
$$F_{\mathrm{QM}}(Q^2) = F_q(Q^2)e^{-Q^2b^2/6} \quad \text{(C3)}$$

are not distinguished seriously from their experimentally measured counterparts used in Eq. (C1):

$$\mu_p = 2.79, \quad \mu_n = -1.91,$$
$$F_2(Q^2) \approx F_{\mathrm{dip}}(Q^2) = \left(\frac{1}{1 + \frac{Q^2}{\Lambda_N^2}}\right)^2. \quad \text{(C4)}$$

It is important to stress here that the quark-model magnetic form factor, as can be seen in Fig. 9, resembles quite precisely the respective nucleon form factor found with the standard dipole fit, in the region $Q^2 \simeq 1$–$2\,\mathrm{GeV}^2/c^2$, that is, near the region of minimum for the deuteron magnetic form factor $B(Q^2)$—see the respective curve in Fig. 9 for the choice of $b = (\sqrt{3/2})r_0 = 0.467$ fm.

Thus, in the nucleon sector, we replace the quark-model current $J^\mu_{N\mathrm{QM}}$ with the standard representation of the nucleon current J^μ_N given by Eqs. (C1) and (C4), and only the nonadditive two-body current (which gives only a small correction to the single-nucleon current J^μ_N) is calculated on the basis of the CQM.

In particular, the CQM technique is used for calculation of the last two terms in Eq. (25). These terms are contributions of the graphs shown in Figs. 6(f) and 6(e), respectively.

(i) For the graph in Fig. 6(f), the diagonal matrix element $\langle \mathrm{DB}|\sum_{i=1}^{6} j_i^\mu \varepsilon_\mu^{(\lambda)}|\mathrm{DB}\rangle$ is reduced here to the matrix element with the s^6 baglike wave functions. This term is found by the same technique as for the nucleon matrix element calculation in Eqs. (C2) and (C3). As a result, for the transverse current component ($\lambda = \pm 1$, $\varepsilon_\mu^{(\lambda)} = \{0, \boldsymbol{\epsilon}^{(\lambda)}\}$) one gets

$$\langle \mathrm{DB}|\sum_{i=1}^{6} j_i^\mu \varepsilon_\mu^{(\lambda)}|\mathrm{DB}\rangle = \langle s^6, S=1, T=0|\sum_{i=1}^{6} j_i^\mu \varepsilon_\mu^{(\lambda)}|s^6, S=1, T=0\rangle = -\frac{(\boldsymbol{\sigma}_p + \boldsymbol{\sigma}_n)\boldsymbol{\epsilon}^{(\lambda)}}{2}\mu_N^s F_{s^6}(Q^2), \quad \text{(C5)}$$

with $F_{s^6}(Q^2) = F_q(Q^2)e^{-5Q^2b^2/24}$ and $\mu_N^s = \mu_p + \mu_n$.

(ii) With the graph in Fig. 6(e), the transition matrix element $NN \to \mathrm{DB}$ can be found similarly to Eq. (4), that is, by using the expansion over the six-quark shell-model states with restriction by the most important low-lying states:

$$\begin{aligned}\langle d(NN)|\sum_{i=1}^{6} j_i^{\mu}\varepsilon_{\mu}^{(\lambda)}|\mathrm{DB}\rangle &= \sum_{n=2,4,6}\sum_{f}\int u(r)\langle N(123)| \\ &\times \langle N(456)|s^{6-n}p^{n}\{f\}\rangle dr \\ &\times \langle s^4p^2\{f\}\,|\sum_{i=1}^{6} j_i^{\mu}\varepsilon_{\mu}^{(\lambda)}|\,s^6\rangle \\ &= -\frac{(\boldsymbol{\sigma}_p+\boldsymbol{\sigma}_n)\boldsymbol{\epsilon}^{(\lambda)}}{2} \\ &\times \sum_{n}\langle u|nS(NN)\rangle \\ &\times \sum_{f} C_{nf}F_{s^6-s^{6-n}p^n}(Q^2).\end{aligned} \tag{C6}$$

Here

$$F_{s^6-s^4p^2}(Q^2) = \frac{1}{5}F_q(Q^2)\left(-\frac{5Q^2b^2}{24}\right)e^{-5Q^2b^2/24},$$

$$F_{s^6-s^4p^2}(Q^2) = \frac{1}{25}F_q(Q^2)\left(-\frac{5Q^2b^2}{24}\right)^2 e^{-5Q^2b^2/24},$$

$$F_{s^6-s^4p^2}(Q^2) = \frac{1}{125}F_q(Q^2)\left(-\frac{5Q^2b^2}{24}\right)^3 e^{-5Q^2b^2/24},$$

and

$$\langle u|nS(NN)\rangle = \int_0^{\infty} u(r)\varphi_{nS}(r)\,dr,$$

where the factors $1/5$, $1/25$, and $1/125$ are fractional parentage coefficients (f.p.c.) of the translational-invariant quark shell model (see [51,71] for details) for the most important (symmetric in the coordinate space) Young tableaux $[f_X] = [6]$. The full table of the f.p.c. (including the C_{nf}) taken into account in the calculation of the right-hand side of Eq. (C6) will be published elsewhere.

APPENDIX D: DEUTERON $M1$ AND $E2$ TRANSITION AMPLITUDES

The $M1$ and $E2$ amplitudes that are used for the cross-section calculation in Eqs. (36) and (37) take the following form [separately for the spin (s) and convection (c) current components]:

$$M1^{(\lambda)I=1}_{MM'}(s) = \delta_{M',-\lambda}\,\delta_{M,0}\,(\mu_n-\mu_p)\,\lambda\left(\frac{-ieq}{2m_N}\right)I_0\big(u,{}^1S_0\big), \tag{D1}$$

$$\begin{aligned}M1^{(\lambda)I=0}_{MM'}(s) &= \delta_{M',M-\lambda}\,(\mu_n+\mu_p)[\lambda\sqrt{2}(1M1\,-\lambda) \\ &\times |1(M-\lambda)]\left(\frac{-ieq}{2m_N}\right)\left\{I_0\big(u,{}^3S_1\big)-\frac{1}{2}I_0\right. \\ &\times \big(w,{}^3D_1\big)+\frac{1}{\sqrt{2}}I_2\big(uw,{}^3S_1{}^3D_1\big) \\ &\left.+\frac{1}{2}I_2\big(w,{}^3D_1\big)\right\},\end{aligned} \tag{D2}$$

$$\begin{aligned}M1^{(\lambda)I=0}_{MM'}(c) &= \delta_{M',M-\lambda}[\lambda\sqrt{2}(1M1\,-\lambda)|1(M-\lambda)]\left(\frac{-ieq}{2m_N}\right) \\ &\times \frac{3}{8}\big\{I_0\big(w,{}^3D_1\big)+I_2\big(w,{}^3D_1\big)\big\},\end{aligned} \tag{D3}$$

$$\begin{aligned}E2^{(\lambda)}_{MM'}(s) &= \delta_{M',M-\lambda}(\mu_n+\mu_p) \\ &\times \left[-\frac{\sqrt{10}}{\sqrt{3}}(1M2\,-\lambda)|1(M-\lambda)\right]\left(\frac{-ieq}{2m_N}\right) \\ &\times \frac{3}{\sqrt{2}}I_2\big(uw,{}^3S_1{}^3D_1\big),\end{aligned} \tag{D4}$$

$$\begin{aligned}E2^{(\lambda)}_{MM'}(c) &= \delta_{M',M-\lambda}[\lambda\sqrt{2}(1M1\,-\lambda)|1(M-\lambda)]\left(\frac{-ieq}{2m_N}\right) \\ &\times \frac{3}{8}\big\{I_0\big(w,{}^3D_1\big)+I_2\big(w,{}^3D_1\big)\big\},\end{aligned} \tag{D5}$$

where I_0 and I_2 are the following overlap integrals:

$$\begin{aligned}I_0(f,Z) &= \int_0^{\infty} f(r)Z(r,p_n)j_0(qr/2)\,dr, \\ I_2(f,Z) &= \int_0^{\infty} f(r)Z(r,p_n)j_2(qr/2)\,dr, \\ I_2\big(uw,{}^3S_1{}^3D_1\big) &= \frac{1}{2}\int_0^{\infty}[u(r){}^3D_1(r,p_n) \\ &\quad + w(r){}^3S_1(r,p_n)]\,j_2(qr/2)\,dr.\end{aligned} \tag{D6}$$

Here $Z(r,p_n)$ can be any of the scattering wave functions in the ${}^1S_0$, ${}^3S_1$, or ${}^3D_1$ channels.

For the sake of convenience, the factors that are equal to unity on modulo are separated out in square brackets:

$$\begin{aligned}\lambda\sqrt{2}(1M1\,-\lambda)|1(M-\lambda) &= 1, \\ -\frac{\sqrt{10}}{\sqrt{3}}(1M2\,-\lambda)|1(M-\lambda) &= (-1)^M.\end{aligned} \tag{D7}$$

When summed over the M and λ induces, these terms play a role similar to the Kroneker delta.

[1] A. N. Bazhenov, L. A. Grigor'eva, V. V. Ivanov, E. A. Kolomensky, V. M. Lobashev, V. A. Nazarenko, A. N. Pirozhkov, and Y. V. Sobolev, Phys. Lett. **B289**, 17 (1992); V. A. Vesna, E. A. Kolomensky, V. P. Kopeliovich, V. M. Lobashev, V. A. Nazarenko, A. N. Pirozhkov, and E. V. Shulgina, Nucl. Phys. **A352**, 181 (1981).

[2] T. M. Müller, D. Dubbers, P. Hautle, E. I. Bunyatova, E. I. Korobkina, and O. Zimmer, Nucl. Instrum. Methods Phys. Res. A **440**, 736 (2000).

[3] S. Aufret *et al*., Phys. Rev. Lett. **54**, 649 (1985).

[4] R. G. Arnold *et al*., Phys. Rev. Lett. **58**, 1723 (1987).

[5] D. Abbot *et al*. (The Jefferson Lab t_{20} Collaboration), Phys. Rev. Lett. **82**, 1379 (1999).

[6] D. R. Phillips, S. J. Wallace, and N. K. Devine, Phys. Rev. C **72**, 014006 (2005).

[7] E. Hummel and J. A. Tjon, Phys. Rev. Lett. **63**, 1788 (1989); Phys. Rev. C **42**, 423 (1990); **49**, 21 (1994).

[8] R. Schiavilla, Phys. Rev. C **72**, 034001 (2005).

[9] W. P. Sitarski, P. G. Blunden, and E. L. Lomon, Phys. Rev. C **36**, 2479 (1987).

[10] H. Arenhövel, F. Ritz, and T. Wilbois, Phys. Rev. C **61**, 034002 (2000).

[11] J. Carlson and R. Schiavilla, Rev. Mod. Phys. **70**, 743 (1998).

[12] D. O. Riska, Phys. Scripta **31**, 471 (1985); Phys. Rep. **181**, 207 (1989).

[13] L. E. Marcucci, M. Viviani, R. Schiavilla, A. Kievsky, and S. Rosati, Phys. Rev. C **72**, 014001 (2005).

[14] T.-S. Park, K. Kubodera, D.-P. Min, and M. Rho, In *Nuclear Physics with Effective Field Theory II*, Proceedings from the Institute for Nuclear Theory, Vol. 9, edited by P. F. Bedaque, M. P. Savage, R. Seki, and U. vanKolk (World Scientific, Singapore, 2000), p. 368; arXiv:nucl-th/9904053.

[15] J.-W. Chen, G. Rupak, and M. J. Savage, Phys. Lett. **B464**, 1 (1999).

[16] G. Breit and M. L. Rustgi, Nucl. Phys. **A161**, 337 (1971).

[17] K. Kubodera, J. Delorme, and M. Rho, Phys. Rev. Lett. **40**, 755 (1978).

[18] T.-S. Park, D.-P. Min, and M. Rho, Phys. Rep. **233**, 341 (1993).

[19] T.-S. Park, D.-P. Min, and M. Rho, Phys. Rev. Lett. **74**, 4153 (1995); Nucl. Phys. **A596**, 515 (1996).

[20] R. Schiavilla and V. R. Pandharipande, Phys. Rev. C **65**, 064009 (2002).

[21] I. T. Obukhovsky, D. Fedorov, A. Faessler, T. Gutsche, and V. E. Lyubovitskij, Phys. Lett. **B634**, 220 (2006).

[22] D. Plümper, J. Flender, and M. F. Gari, Phys. Rev. C **49**, 2370 (1994).

[23] V. I. Kukulin, I. T. Obukhovsky, V. N. Pomerantsev, and A. Faessler, J. Phys. G **27**, 1851 (2001).

[24] A. P. Burichenko and I. B. Khriplovich, Nucl. Phys. **A515**, 139 (1990).

[25] V. I. Kukulin, I. T. Obukhovsky, V. N. Pomerantsev, and A. Faessler, Int. J. Mod. Phys. E **11**, 1 (2002).

[26] V. I. Kukulin and M. A. Shikhalev, Phys. At. Nucl. **67**, 1558 (2004).

[27] A. Faessler, V. I. Kukulin, and M. A. Shikhalev, Ann. Phys. (NY) **320**, 71 (2005).

[28] Y. Yamauchi and M. Wakamatsu, Nucl. Phys. **A457**, 621 (1986).

[29] M. Oka and K. Yazaki, Nucl. Phys. **A402**, 477 (1983).

[30] E. M. Henley, L. S. Kisslinger, and G. A. Miller, Phys. Rev. C **28**, 1277 (1983); K. Bräuer, E. M. Henley, and G. A. Miller, *ibid*. **34**, 1779 (1986).

[31] A. Buchmann, Y. Yamauchi, and A. Faessler, Nucl. Phys. **A496**, 621 (1989).

[32] A. P. Kobushkin, Phys. At. Nucl. **62**, 1140 (1999).

[33] F. Wang, J.-L. Ping, G. H. Wu, L.-J. Teng, and T. Goldman, Phys. Rev. C **51**, 3411 (1995).

[34] H. Pang, J. Ping, F. Wang, T. Goldman, and E. Zhao, Phys. Rev. C **69**, 065207 (2004).

[35] T. Goldman, K. Maltman, G. J. Stephenson, K. E. Schmidt, and F. Wang, Phys. Rev. C **39**, 1889 (1989).

[36] H. Pang, J. Ping, L. Chen, F. Wang, and T. Goldman, Phys. Rev. C **70**, 035201 (2004).

[37] S.-I. Ando and C. H. Hyun, Phys. Rev. C **72**, 014008 (2005).

[38] S. R. Beane, P. F. Bedaque, M. J. Savage, and U. van Kolk, Nucl. Phys. **A700**, 377 (2002).

[39] S. Fleming, T. Mehen, and I. W. Stewart, Nucl. Phys. **A677**, 313 (2002).

[40] S. Ishikawa, M. Tanifuji, Y. Iseri, and Y. Yamamoto, Phys. Rev. C **69**, 034001 (2004).

[41] A. S. Khrykin, Nucl. Phys. **A721**, 625c (2003); nucl-exp/0211034.

[42] P. A. Zolnierczuk, T. P. Gorringe, M. D. Hasinoff, M. A. Kovash, S. Tripathi, and D. H. Wright, Phys. Lett. **B549**, 301 (2002); P. A. Zolnierczuk (RMC Collaboration), Acta Phys. Polon. B **31**, 2349 (2000).

[43] V. I. Kukulin, V. N. Pomerantsev, M. Kaskulov, and A. Faessler, J. Phys. G **30**, 287 (2004); V. I. Kukulin, V. N. Pomerantsev, and A. Faessler, J. Phys. G **30**, 309 (2004).

[44] N. Kaiser, R. Brockman, and W. Weise, Nucl. Phys. **A625**, 758 (1997); N. Kaiser, S. Gerstendorfer, and W. Weise, *ibid*. **A637**, 395 (1998).

[45] E. Oset, H. Toki, M. Mizobe, and T. T. Takahashi, Prog. Theor. Phys. **103**, 351 (2000).

[46] M. M. Kaskulov and H. Clement, Phys. Rev. C **70**, 014002 (2004).

[47] O. Krehl, C. Hanhart, C. Krewald, and J. Speth, Phys. Rev. C **62**, 025207 (2000).

[48] B. D. Serot and J. D. Walecka, Adv. Nucl. Phys. **16**, 1 (1986); B. D. Serot, Rep. Prog. Phys. **55**, 1855 (1992).

[49] M. Cristoforetti, P. Faccioli, G. Ripka, and M. Traini, Phys. Rev. D **71**, 114010 (2005).

[50] M. Harvey, Nucl. Phys. **A352**, 301 (1981); **A481**, 834(E) (1988).

[51] A. M. Kusainov, V. G. Neudatchin, and I. T. Obukhovsky, Phys. Rev. C **44**, 2343 (1991); I. T. Obukhovsky, Prog. Part. Nucl. Phys. **36**, 359 (1996).

[52] F. Stancu, S. Pepin, and L. Y. Glozman, Phys. Rev. C **56**, 2779 (1997); D. Bartz and F. Stancu, *ibid*. **63**, 034001 (2001).

[53] C. van der Leun and C. Alderliesten, Nucl. Phys. **A380**, 261 (1982).

[54] A. Huber, T. Udem, B. Gross, J. Reichert, M. Kourogi, K. Pachucki, M. Weitz, and T. W. Hänsch, Phys. Rev. Lett. **80**, 468 (1998).

[55] T. E. O. Ericson and M. Rosa-Clot, Nucl. Phys. **A405**, 497 (1983).

[56] D. M. Bishop and L. M. Cheung, Phys. Rev. A **20**, 381 (1979).

[57] I. Lindgren, in *α-, β-, and γ-Ray Spectroscopy*, Vol. 2, edited by K. Siegbahn (North-Holland, Amsterdam, 1965), p. 1620.

[58] J. J. de Swart, C. P. F. Terheggen, and V. G. J. Stocks, University of Nijmegen Report, 1995, nucl-th/9509032.

[59] J. Horáček, J. Bok, V. M. Krasnopolsky, and V. I. Kukulin, Phys. Lett. **B172**, 1 (1986).

[60] M. M. Kaskulov, P. Grabmayr, and V. I. Kukulin, Int. J. Mod. Phys. E **12**, 449 (2003).

[61] D. Abbott *et al*. (The JLab t_{20} Collaboration), Eur. Phys. J. A **7**, 421 (2000); B. Boden *et al*., Z. Phys. C **49**, 175 (1991); M. Bouwhuis *et al*., Phys. Rev. Lett. **82**, 3755 (1999); V. F. Dmitriev *et al*., Phys. Lett. **B157**, 143 (1985); M. Ferro-Luzzi *et al*., Phys. Rev. Lett. **77**, 2630 (1996); M. Garçon *et al*., Phys. Rev. C **49**, 2516 (1994); R. Gilman *et al*., Phys. Rev. Lett. **65**, 1733 (1990); M. E. Schulze *et al*., *ibid*. **52**, 597 (1984).

[62] V. G. J. Stoks, R. A. M. Klomp, C. P. F. Terheggen, and J. J. de Swart, Phys. Rev. C **49**, 2950 (1994).

[63] T.-S. Park, K. Kubodera, D.-P. Min, and M. Rho, Phys. Lett. **B472**, 232 (2000).

[64] A. Akhiezer and V. B. Berestetski, *Quantum Electrodynamics* (Wiley, New York, 1963).

[65] J. M. Eisenberg and J. W. Greiner, *Nuclear Theory*, Vol. 2, *Excitation Mechanisms of the Nucleus, Electromagnetic and Weak Interactions* (North-Holland, Amsterdam, 1970).

[66] A. R. Edmonds, *Angular Momentum in Quantum Mechanics* (Princeton University Press, Princeton, NJ, 1957).

[67] I. L. Grach and M. Zh. Shmatikov, Sov. J. Nucl. Phys. **45**, 579 (1986).

[68] E. A. Strokovsky, Phys. At. Nucl. **62**, 1120 (1999).

[69] D. L. Groep *et al*., Phys. Rev. C **63**, 014005 (2001); D. P. Watts *et al*., *ibid*. **62**, 014616 (2000); L. Weinstein *et al*. (CLAS Collaboration), Eur. Phys. J. A **19**, SL, 175 (2004).

[70] I. T. Obukhovsky, V. G. Neudatchin, Y. F. Smirnov, and Y. M. Chuvilsky, Phys. Lett. **B88**, 231 (1979).

[71] I. T. Obukhovsky, V. I. Kukulin, M. M. Kaskulov, P. Grabmayr, and A. Faessler, J. Phys. G **29**, 2207 (2003).